Lunar Landing and Launching Pad Design Considerations Using ISRU Materials

Eliza Mount[*], Monique Hollister[*], Christina McNichol[*],
Shirley J. Dyke[**], Julio A Ramirez[*], Akanshu Sharma[*], Antonio Bobet[*]
[*]Lyles School of Civil and Construction Engineering
[**]School of Mechanical Engineering
Purdue University, West Lafayette, IN, 47907, USA

Abstract: Launching and landing pads (LLPs) will be essential elements to serve a future lunar base. There is widespread acceptance that these structures will be manufactured from in situ materials. Structural materials made from these indigenous materials are expected to be brittle. Thus, they will exhibit the typical diverse behaviors and inherent variabilities in properties that are common in indigenous construction materials. Hard-won lessons on how to design reliable structures from brittle materials on the Earth need to be leveraged. It should be noted that earlier examples of these applications resulted in massive structures. It was not until Portland cements, other cementitious materials, chemical admixtures, steel, and more recently carbon fiber-based elements became available, and in general, composites were better understood, that more elegant and slender structures were realized. In this research, we adapt and apply well-established methodologies used for slab-on-grade construction toward the development of a design framework for lunar LLPs. The structural considerations in designing such a slab are discussed in detail starting from first principles and unknown initial dimensions to illustrate their impact on the design. This approach is necessary given the low state of entropy of the knowledge with respect to performance and actual material properties in such extreme environments. It is demonstrated through an illustrative example in which we design an LLP using the best available information and properties for sintered lunar regolith. Additional information that will need to be obtained or verified through in situ testing is also defined. The example design is intended to service spacecraft of up to 50 tons. The dimensions used for the loads represent spacecraft being developed at the present time for transporting cargo and supplies to the surface of the Moon. The application of a wealth of fundamental knowledge, practical experience, and technologies will be essential for the design and construction of resilient and sustainable infrastructure on the Moon and other similarly challenging environments. The paper concludes with a discussion of the path forward to design and realize such construction on the Moon.

1. Introduction

NASA and its partner agencies have the goal of expanding U.S. human space flight operations to the Moon and supporting a sustained human presence [1]. A critical aspect of both exploring the Moon and developing a sustainable lunar economy is having the necessary infrastructure to ensure reliable, safe, and consistent delivery of equipment and consumables to the lunar surface, as well as launching payloads and crew to lunar orbits [2]. Constructing the right type of infrastructure would enable repeated landings and launches of a variety of spacecraft with different payload sizes [3, 4] while supporting the objective to perform precision landing [5]. Ideally, all this activity will take place without significant damage to the LLP, or to any other infrastructure on the lunar surface or in cislunar space.

On the Earth, landing and launch pads have traditionally been monolithic structures. These structures are designed to withstand enormous forces and extreme temperatures, and are subjected to chemicals and other spills that may harm or weaken that structure over time. This type of construction is possible because we have well over one-hundred years of experience with an indigenous composite material, reinforced concrete. Engineers, using concrete in combination with steel reinforcement, have constructed some of the world's tallest and most impressive structures such as the Burj Khalifa [6]. This

combination of a brittle material (concrete) and a ductile one (steel) into a powerful composite that takes advantage of the best properties of both has led to structural concrete being the most utilized construction material on Earth. Design with structural concrete throughout the full range of utilization, from plain (without reinforcement) to fully prestressed (with the use of high strength steel) has evolved immensely, guided by user needs, new materials, improved load estimations, and cost [7].

Such broad and reliable utilization is due to the valuable lessons that have been derived from both the large number of laboratory tests conducted around the world and the field observations that are essential for full-scale structural systems that are too large to test in a laboratory. Data compiled and knowledge developed provides the engineering knowhow to deal with the inherent variabilities of concrete and generate safe design procedures. Reinforcement is recognized as being needed to control cracking under tensile loads and temperature expansions. Engineers have established an understanding of how to characterize the substrate (soil), and how to design to avoid negative interactions between the substrate and the structure. Reliable design and construction on the Earth have been possible because civil engineers understand the material's behavior and variability, and have established standard tests for confirming that the strength and durability meet the design expectations [8]. Furthermore, on the Earth, we can examine the site prior to construction to make assessments both at the surface and below the surface.

Clearly, little to no experience like this exists related to design and construction of large scale civil or military infrastructure on any extraterrestrial body. The lunar environment is significantly more extreme than any natural environment on the Earth, and the construction of reliable infrastructure will require that we acquire much of the same understanding and hard-won lessons we have for Earth-construction. Jehn and Dreyer described and demonstrated a method for analyzing an LLP using a finite element analysis [9]. They proposed a 1.0 m thick LLP and then described how the estimated loads would result in deflections and deformation in the pad. They also discussed some of the failure modes as well as the data and information that would be needed to perform the design process. Metzger and Mantovani studied potential trajectories for ejecta kicked up by a rocket plume during a typical landing of a 40-ton lander in loose lunar regolith [11]. They found that, based on current information, ejecta would be likely to escape the gravitational field of the Moon and would thus pose a risk to vehicles in cislunar orbits. This expectation agrees with the observations of the Apollo astronauts [2]. However, finite element analysis requires estimation of initial dimensions and material properties. Assuming initial dimensions and properties without the use of first principles could hide potential modes of failure and interactions critical to achieve a safe and efficient design. This point will be illustrated in the next sections of this paper.

Once we have the necessary information, the selection of a construction material or method for construction of an LLP should depend on multiple aspects, including equipment needs, costs to transport any required materials from Earth, energy required, construction time, life-cycle maintenance and repair expected, etc. However, the indigenous materials made of regolith that will potentially serve as structural materials have yet to be characterized at scale for structural strength, or mechanical and chemical durability [8]. The relevant information about the subsurface is not known – specifically the engineering properties and the ability to improve them – to the level of detail and reliability needed to accommodate design and construction. Leveraging all the fundamental knowledge, practical experience, and technologies used for similar construction on the Earth must thus be exploited to construct sustainable and safe LLPs and other structures on the Moon.

In a trade study considering manufactured ISRU construction methods that incorporated many of these metrics, microwave sintering was identified as the most favorable method to construct a lunar landing pad [12]. Additionally, microwave and laser sintered materials have been targeted by recent NASA funding, such as the Moon-to-Mars Planetary Autonomous Construction Technology (MMPACT) Project [13]. NASA's Marshall Space Flight Center and ICON, a private company, are

studying microwave and laser sintered materials, respectively. They have also obtained a set of preliminary values for material properties needed for design. Although the manufacturing process is energy intensive, these classes of sintered regolith materials are viewed as promising candidates for full-scale ISRU construction.

Based on the current expectation that sintered regolith will be the most probable option as a structural material, and the availability of a more comprehensive set of preliminary values for the needed material properties, the illustrative LLP example included in this paper will consider this material. The application of first principles of mechanics and strength of materials in the design is adopted to illustrate how fundamental assumptions affect the design outcome and introduce potentially competing objectives between LLP design choices. As these structures are realized, in situ testing will arguably be essential to develop the knowledge and gain the experience needed to design and construct structures in this extreme environment.

This paper is focused on developing a design framework for LLPs using an ISRU-based structural material. An illustrative example is included that leverages the extensive amount of basic knowledge and experience related to the design of structural concrete slabs supported directly by the natural (native) ground surface, or by a prepared and compacted subbase and subgrade, as shown in Fig. 1. This type of structural slab is commonly employed in highway pavements, airport runways, and industrial floors on the Earth. Although the design of this class of structures is common and appropriate, and safe design procedures are available, the performance of LLPs on the Earth relies on the presence of ductile steel reinforcement acting compositely with the concrete. However, this approach is not now an option for the Moon. LLP design under these extreme conditions and with these new materials is not straightforward. To properly deal with the various solicitations associated with the spacecraft loads, extreme temperatures, and plume-structure interactions, the design process requires weighing certain competing objectives that will be discussed herein. Several assumptions will also need to be verified and data will need to be collected both before construction of the LLP and while it is in service [8, 9, 10].

The paper is organized as follows. Section 2 describes the relevant knowledge, considerations, and methods to consider when designing and constructing an LLP using ISRU materials. This information is brought together to propose the design framework. First principles are adopted, and in some instances, procedures on the Earth are compared to those for the Moon. These comparisons are made to identify areas of commonality, and more importantly to identify where gaps may exist and the type of data needed to fill those gaps. Section 3 provides the specific details needed for design, such as relevant conditions at the chosen location on the Moon, and the best information that is known to date about sintered regolith material. Section 4 walks through an illustrative numerical example to demonstrate the design procedure for an LLP and to then analyze the designed structure under service loads. Section 5 critically examines the information that is either still needed, or must be further verified, to design such a structure and begin planning other structures to be constructed of ISRU materials. Section 6 concludes with recommendations on a path forward to realize ISRU-based construction of infrastructure in extraterrestrial environments.

2. Considerations in the Design of Slabs-on-Ground

The typical arrangement for Earth-surface structural slabs-on-ground, as well as those to be executed on the surface of the Moon through ISRU, is shown in Fig. 1. The prepared subbase consists of gravel and is between 8 in (203 mm) and 16 in (406 mm) thick. This subbase, or subgrade, typically serves to improve the slab support more uniformly, compared to what would be provided by the natural ground. This subbase is compacted and may be topped with sand, and often a waterproof membrane. In construction on Earth, this membrane consists of asphalt-impregnated paper, used to avoid the loss of fines from the concrete when it is cast, and most importantly, to reduce the friction between the slab and the subbase. Construction of such a structure using sintered regolith on the surface of the Moon may not

require such protection against freeze-thaw action in the absence of water or leaking of fines (the smaller particles) into the subbase. The friction between the sintered regolith pad and the subbase is still an important consideration for the design of the pad. Reinforcement consisting of welded wire fabric or reinforcing bars is used to control cracking of the pad due to thermal effects and friction. However, it is not always used and is not expected to be included for a sintered regolith slab. The slab rests on top of these layers.

Structural material properties must be quantified in a dependable manner to design any structure. For the design of an LLP, at least compressive strength, tensile strength, modulus of elasticity, Poisson's ratio, and coefficient of thermal expansion of the construction material should be known. The behavior and properties of the structural materials anticipated to be manufactured from indigenous lunar regolith are not well understood at this time, but are generally assumed to be brittle. It is logical to assume that these brittle structural materials will be significantly weaker in tension than in compression. Aside from basic material properties of the LLP, the characteristics of the subsurface material must be known. In addition, the coefficient of friction between the compacted regolith and the material is important. Time-dependent properties such as creep and the effect of cycles of low and high temperature are also important if one aims to establish longer term or life-cycle performance, inspection-related needs, and possible interventions to maintain and repair the LLP for adequate service performance.

Structural design becomes a series of choices depending on material and structural properties, fundamental structural and material behavior, and the loading demands. A variety of factors must be considered to determine the design of the LLP, including thermal changes and gradients, friction between the subbase and the pad, the subbase characteristics, the effects of self-weight and heavy concentrated loads, the presence or absence of reinforcement, and plume loads. At the present, little is known about the indigenous materials that will be used on the Moon. While the design procedure described in this paper is sound and important issues and trades that need to be considered are raised, the specific numbers that result from the procedure may change once a more complete understanding of the materials becomes available.

Structures designed for the Earth benefit from collecting extensive data that quantify both the service loads and variability in materials. All of that information is encoded in design methods, such as LRFD (Load and Resistance Factor Design) [14]. Without the availability of similar data, in this work we rely on first principles. The proposed design approach is thus based on allowable stresses and service loads. This approach is selected to allow a robust definition of the factor of safety used in its design. As the knowledge of the properties of the material used and design conditions are in a low level of entropy, the factor of safety utilized in its design gains importance. While the design is conducted using ISRU, the procedure provides a framework for design with other materials. Note that this approach is meant to design the LLP to withstand expected demands without experiencing cracking. In the illustrative example in Section 4, the LLP is assumed to be built from sintered regolith, and the design objective is to keep it uncracked under service loads, making it behave more like a rigid pavement instead of a flexible one. We also assume that the slab is homogenous, isotropic, elastic, and is assumed to be square.[1]

2.1 Thermal Effects and Considerations

Thermal effects may be the most critical loads to consider for the design of an LLP. Thermal conditions due to the environment will cause changes and gradients leading to expansions and contractions. On the Moon, exposure to the 28-day "Lunar day" alone will cause significant stresses in the LLP. In addition, rocket plumes will create short term thermal gradients throughout the pad that will reach much higher localized temperatures. These loads are likely to be the most destructive solicitation expected with this

[1] Note that some of the equations are empirical and thus require that specific units be used. Those units are specified near the relevant equation.

structure. However, there is an interplay between the effects of different loadings that ultimately will require that certain trade-offs be made in the design of the LLP, as we will demonstrate later in Section 5. In this section we specifically consider the stresses induced by the thermal expansion and contraction associated with temperature variations associated with a Lunar cycle.

Figure 2(a) shows a slab-on-ground, unloaded except for its own weight. Axial deformations may be induced in such a structure by restrained shrinkage (during curing, for concrete on the Earth). However, as the materials to be potentially used for an LLP are not likely to contain water, the more relevant case to consider is temperature effects. Axial expansion of the slab will clearly occur when there is an increase in temperature. No matter what the source of the deformation, such expansion is resisted by frictional drag between the slab and the subgrade, causing a tensile force in the slab, as shown in Fig. 2(b). Due to the expected behavior of brittle materials, expansion (tension) is a more critical case than contraction (compression), and we examine that case herein.

Consider a strip of the slab having a unit width and experiencing an increase in temperature that causes expansion of the slab. Let *L* be the total length of the slab, and *h* be the slab thickness. Equilibrium of the horizontal forces for half the length on a unit strip (Fig. 2(c)) results in a tensile force at the cross-section at *L*/2 given by

$$T = (w_0 \mu L)/2 \tag{1}$$

where w_0 is the self-weight of the slab, μ is the coefficient of friction between the slab and subbase, and T is the tensile force per unit width.

The potential for restrained, temperature-induced deformation raises important questions for the LLP, such as whether construction joints should be considered, as well as bond-breakers between the pad and subgrade. Other important considerations are the thermal coefficient of sintered regolith, the friction coefficient between the sintered regolith pad and the subgrade, and the tensile strength of the sintered regolith pad.

In the case of a concrete slab-on-grade, the coefficient of friction varies widely as a function of the roughness of the subgrade, and tests show a range between 1 and 2.5 [15]. Researchers have obtained values for the coefficient of friction [16] for a variety of different typical construction materials. By testing 5 in (125 mm) thick slabs placed on different base materials, μ values obtained were well over 3 for an asphalt surface, while a blended washed sand and gravel mix produced a value just under 2, and a simple sand subbase yielded a value just under 1. It is possible to achieve values less than 1 if a bond-breaker element is used between the slab and subgrade. Note that after the first movement (first full thermal expansion of the pad), the value of μ may decrease for some combinations of materials, and thus less friction would be present during subsequent movements. We will assume a more typical value of 1.5, which is also recommended by AASHTO (American Association of State Highway and Transportation Officials) [17]. This value should be obtained for the actual materials to be used.

Assuming uncracked-section behavior, the tensile force T will result in a tensile stress, f_t, at the top of the slab (psi per foot of slab width) given by

$$f_t = T/[12 * h]. \tag{2}$$

More often, there is a variation of temperature throughout the slab thickness rather than a uniform change. For instance, the exposed top surface may contract more than the bottom due to a rapid drop in temperature, leading to a tendency of the slab section to curl up. This curling-up effect is the consequence of different strain values at the top and bottom of the slab, e_{t1} and e_{t2}, respectively. This behavior is shown in Fig. 3(a), where $e_{t1} > e_{t2}$, representing a shortening from the undeformed vertical section. The strain distribution for this case is labeled "free shrinkage thermal strain diagram" in Fig. 3(b).

Sometimes the self-weight of the slab prevents this curling-up, resulting in a uniform distribution of strain, shown in Fig. 3(b) by the vertical dashed line labeled "uniform strain surface." Restraining the

pad in this way results in warping stresses as shown in Fig. 3(b). Note that these effects occur in both horizontal directions, longitudinal (direction 1) and transverse (direction 2), as shown in the top view in Fig. 3(c). For this state of stress, assuming linear elastic behavior, the tensile strain in direction 1, e_1, is calculated as

$$e_1 = (f_1 - \nu f_2)/E_c \tag{3}$$

where E_c is the elastic modulus, and ν is Poisson's ratio, both for the LLP material. Note that for a square LLP there is a symmetric temperature profile, $f_1 = f_2 = f_{dt}$, according to Figs. 4(b) and (c). The flexural strain at the top surface is

$$e_1 = [e_{t1} - e_{t2}]/2. \tag{4}$$

The value needed for design is the tensile stress at the surface of the slab due to the variation temperature between the top and bottom surfaces f_{dt}. Substituting Eq. (4) into Eq. (3) results in

$$f_{dt} = e_1 E_c/(1 - \nu) \tag{5}$$

where e_1 is the difference in strain between the top and bottom of the slab, and f_{dt} is the tensile stress due to warping tendency. To determine the total stress induced by these conditions, the warping stress given by Eq. (5) is superimposed on the tensile stress value obtained from Eq. (2) for a uniform temperature change.

2.2 Subgrade/Subbase Considerations

Before we can consider the effects of concentrated loads from spacecraft and other vehicles, it is necessary to consider the behavior of the slab-on-ground, following the work of Westergaard [18, 19]. Assume that the slab on the surface of the Moon is unreinforced and uncracked. Regarding the subgrade, one of two assumptions are made for purposes of design.

The first assumption to consider is that the subgrade behaves as a liquid. This assumption means that the reaction force of the soil is vertical and proportional to the deflection. The reaction force at each point is independent of the forces and displacements at other points on the LLP; this could similarly be represented as a distributed spring over the length of the LLP. With this approach, the stiffness of the ground per unit length is expressed as the modulus of subgrade reaction, k (Winkler's spring constant). The modulus of subgrade reaction is a conceptual relationship between the pressure applied to the soil, q, and resulting soil deflection, δ, for a plate resting on a uniform distributed elastic support, given as

$$k = \frac{q}{\delta}. \tag{6}$$

An alternate approach is to assume that the subgrade behaves as a semi-infinite elastic homogeneous and isotropic solid, such that a concentrated load in one location on the surface of the concrete slab causes vertical displacements everywhere, according to the Boussinesq equation [18, 19]. In practice, the first of the two approaches has been used extensively. Given the lack of hard data and the resulting uncertainty associated with the in situ properties of the lunar surface, the first approach will be used herein to design the LLP.

Note that the physical relationship between load and soil deformation is nonlinear and k is not a fundamental soil property. Usually with knowledge of soil classification and some local experience, the engineer can assign an appropriate k value and design for the specific soil conditions. After the subgrade soils have been classified, the general range of k values can be approximated from data. As noted earlier, the type of soil structure, density, moisture content, and prior loading determine the load-deformation

relationship. The relationship also depends on the width and shape of the loaded area, depth of the subgrade, and position under the slab. In addition, time may be a significant factor, because any deeper compressible soils may settle due to consolidation, and near-surface soils may settle. The values of k for different soils vary widely depending on the type, relative density, degree of consolidation, and moisture content. The values used are obtained through tests and experience. Nevertheless, the procedures for static nonrepetitive plate load field tests, outlined in ASTMD1196 [20], are often used in practice to estimate k. ACI 360-10R [21] reveals that values of k, depending on the various parameters, can range from 100 to 700 pci. These values would be based on the approximate interrelationships between soil classifications and bearing values [22].

Initially, a wide range of subgrade conditions may exist across the site. The soil-support system is rarely uniform, and some soil work is generally required to produce a more uniform surface to support the slab. After approximating the value of k, the engineer may adjust it based on local experience, expected seasonal changes, and expected construction conditions. With this information, a decision can be made whether to use the existing subgrade, improve it by compaction or stabilization, use a subbase and a base course, or vary the thickness of these layers. The extent of this work, such as the degree of compaction or the addition of a base course, is generally limited by economics. Selection of crushed rock or soils in the "well-graded gravel" and "poorly-graded gravel" groups may appear costly as a base material, but the selection of these materials has distinct advantages. They improve the modulus of subgrade reaction, produce more uniform support, and provide an all-weather working surface to speed-up construction during inclement weather. However, the limited knowledge and experience regarding the Moon's soil conditions, as well as the design of an LLP with sintered regolith which we have negligible experience with, strongly suggests that it will be of great importance to examine the sensitivity of the procedure to determine the slab thickness to the value of the modulus of subgrade reaction.

2.3 Heavy Concentrated Loads

The LLP design should include heavy concentrated loads from spacecraft, cargo vehicles, or other causes. Approaches for handling the effects of concentrated loads follow the same principles as those for beams on elastic foundation, and the work of Westergaard [18, 19]. The approach assumes that the slab is homogenous, isotropic, and elastic. This step in the design is used in this paper to select the initial thickness of the slab.

Westergaard considered three separate conditions based on the position of the load with respect to the slab edges. The three conditions are: (1) heavy concentrated load close to the corner of a large slab, (2) heavy concentrated load a considerable distance from the edges of the slab, and (3) heavy concentrated load at an edge of the slab but a considerable distance from the corner. These three loading conditions are illustrated in Fig. 4.

In Condition 1, a point load P represents the service concentrated load applied at the slab corner (see Fig. 5(a)), and the critical stress is due to the tension at the top surface of the slab. An approximate solution for a 90-degree corner is found. Assuming a section of width $2x$, the bending moment is given by

$$M(x) = Px \tag{8}$$

where x is the distance from the concentrated load to the corner of the LLP. The bending moment per unit of width of the slab is given by

$$\frac{M(x)}{2x} = \frac{Px}{2x} = \frac{P}{2}. \tag{9}$$

The section modulus, S, is determined as

$$S = \frac{I}{y_{top}} = \frac{bh^3}{12 * \frac{h}{2}} = \frac{h^2}{6}.$$

The resulting tensile stress at the top surface of the slab, f_{pt}, can thus be calculated as

$$f_{pt} = \frac{M}{S} = \frac{P}{2} * \frac{6}{h^2} = \frac{3P}{h^2} \tag{10}$$

where b is set to 1 for a unit width of the slab. The service load used in this equation for design is increased by a factor of 1.3 to account for impact, as is typical in highway applications [17]. However, the load is unfactored here for allowable stress design.

Note that Eq. (10) is valid only close to the corner of the slab and for a very small contact area of the applied load. Westergaard [18, 19] derived the expressions for the case of a contact area of radius a (Fig. 5(b)), and considered the modulus of subgrade reaction, k, supporting the slab. In this case, the critical tensile stress at the top of the slab, occurring at a distance $2\sqrt{a_1 Q}$ from the corner of the slab, is determined using

$$f_t = \frac{3P}{h^2}\left[1 - \left(\frac{a\sqrt{2}}{Q}\right)^{0.6}\right] \tag{11}$$

where Q, referred to as the ratio of stiffness values (of the landing pad to the soil), can be calculated as

$$Q = \sqrt[4]{\frac{E_c h^3}{12(1-\nu^2)k}}. \tag{12}$$

Note that Q will be large for a very stiff slab on a soft soil, and small for a flexible slab on a stiff base. Westergaard suggested a typical value of 36 in (9144 mm) for concrete highway pavements, which is adopted here [18, 19].

In Condition 2 (see Fig. 4), when the concentrated load is applied some distance from the edges of the slab, the critical stress will be the tension at the bottom of the slab, and directly under the center of the loaded area. The expression derived for the critical stress is

$$f_{pt} = 0.316\frac{P}{h^2}\left[\log(h^3) - 4\log\left(\sqrt{1.6a^2 + h^2} - 0.675h\right) - \log(k) + 6.48\right]. \tag{13}$$

In Condition 3 (see Fig. 4), when the load is applied at a point along the edge of the slab, the critical stress will be the tensile stress at the bottom of the slab, directly under the load. This expression is

$$f_{pt} = 0.572\frac{P}{h^2}\left[\log(h^3) - 4\log\left(\sqrt{1.6a^2 + h^2} - 0.675h\right) - \log(k) + 5.77\right]. \tag{14}$$

These expressions are part of well-established procedures used for decades for the design of slabs-on-grade. In the case when the tensile stress in the slab from any of Eqs. (11), (13), or (14) exceeds the allowable tensile stress for the LLP material, the solution could be to increase the slab thickness until the three computed values fall below the allowable tensile stress. If reinforcement is used, it is also possible to take the calculated elastic tension stress entirely with the reinforcement.

2.4 Punching Shear

Another potential failure mode that will need to be considered is punching shear associated with a heavy lander. One-way shear or beam-action shear would involve an inclined crack extending across the entire width of the LLP. However, two-way shear or punching shear is modeled by a truncated cone or pyramid-shaped surface around the applied concentrated load. Here, the concentrated load applied by the lander is conservatively taken as the entire lander weight, including its payload, distributed over an area represented by a single circular footpad. This approach assumes that there is some difficulty in landing and one footpad hits first. As already mentioned, the force is increased by 30% to simulate dynamic (impact) effects.

Generally, the punching-shear capacity of a slab will be considerably less than its one-way shear capacity. Using the initial thickness obtained from allowable tensile stresses due to bending, punching shear should be evaluated to determine if such a conical failure surface is developed around the spacecraft footpad. An example of such a failure surface is shown in Fig. 6 for the case of a slab and reinforced concrete column. While column-slab connections in reinforced concrete structures will have reinforcement either to resist flexure, or flexure and punching shear, reinforcement is not likely to be used initially for LLPs. This challenge further highlights the need for an allowable stress design that would ensure the LLP remains uncracked in shear. In a brittle material, such a failure would occur suddenly, and without ductility.

Moe [23] conducted an extensive testing program of 43 square, 6-ft x 6-ft slabs, while varying several parameters, such as the amount and distribution of the reinforcement. He also reported a statistical study considering an additional 260 slabs and footings tested by prior researchers. From these extensive tests, Moe concluded that the critical section for shear is located at the face of the column. ACI-ASCE Committee 326 (now 445) [24] accepted Moe's conclusions but showed that a much simpler design equation could be derived. This option is achieved by considering a critical section $d/2$ away from the face of the column, where d is the effective depth of the slab. This location was referred to as the pseudo-critical section for shear. The simplified version has been incorporated in the ACI Code, which defines the internationally accepted procedure for the design of reinforced concrete structures [25].

Moe found that the shear stress, v_{max}, for the case of a column may be found using

$$v_{max} = \frac{V_{max}}{b_0 d} = \left[15\left(1 - 0.075\frac{r}{d}\right) - 5.25\frac{V_{max}}{V_{flex}}\right]\sqrt{f_c'} \tag{15}$$

where b_0 is the perimeter of the loaded area, r is the radius of the loaded area, V_{max} is the maximum shear force in the slab itself, and V_{flex} is the maximum shear force if flexural failure occurred.
Moe's key conclusions [23] include:

- The critical section governing the shear strength should be measured along the perimeter of the loaded area.
- The shear strength depends on flexural strength.
- The ultimate shear strength is predicted with good accuracy by Eq. (15), in terms of shear stress.
- Inclined cracks develop at loads as low as 50% of the ultimate capacity.

For the case of footings, Moe [23] proposed a modification, given by

$$V_{max} = \left[1 - \left(\frac{r + d}{a_s}\right)^2\right] P_{max} \tag{16}$$

where P_{max} is total load on the loaded area, and a_s is the length of one side of a square footing. Mechanically, the case of a footing is analogous to the landing pad, and thus Eq. (16) should be used, with a_s as the length of one side of the LLP (Fig. 4).

The critical section proposed by Moe [23] is used herein (instead of defining the location at $d/2$), as we assume that the LLP will not benefit from the presence of flexural or shear reinforcement. Additionally, due to the lack of transverse reinforcement, $V_{max}/V_{flex} = 1.0$, is used. Finally, because no shear reinforcement is used, only 50% of the calculated strength will be used to check the thickness. Other adaptations are that the effective depth is taken as $d = 0.9h$, and the typical expression of $4\sqrt{f_c'}$ will be used as the upper limit of the diagonal tensile strength in shear (as in reinforced concrete slab design).

Note here that we are assuming these relationships, specifically Eq. (16), empirically developed for punching shear in terrestrial reinforced concrete structures, will hold for ISRU materials used on the Moon. This represents a major assumption that must be tested and verified. The check for punching shear will be performed using these expressions in Section 5.

2.5 Reinforcement

To control cracking associated with shrinkage and temperature in slabs-on-ground, it is common practice across the United States to place reinforcement in the form of welded wire fabric in a concrete slab. Note that this will control cracking, but typically does not prevent cracking. If the slab has cracked at service loads, all the tensile force would likely be assumed to be resisted by the steel working at a specified stress level, f_s. Thus, $T = A_s f_s$, where A_s is the area of steel needed per foot of width of slab in the transverse direction (or, if the LLP is square, in both directions), is given as

$$A_s = \frac{w_0 \mu L}{2 f_s}. \tag{17}$$

This equation provides the basis for estimating the required reinforcement. In U.S. practice, when allowable (specified) stress design is used, it is customary to use a value of f_s of 30 ksi at around 50% of the yield strength of specified grade 60 steel (60 ksi). A design option may be to take the calculated elastic tension stress entirely with the reinforcement. Usually, the reinforcement is taken as 40% of the reinforcement yield strength but not to exceed 24 ksi, placed at the centroid of the calculated tensile stress block it replaces.

It should be noted that in design on the Earth, warping stresses are typically neglected, and the sole function of the reinforcement is to control the width of the crack.

Remarks: Design using the brittle indigenous materials that are expected to be used for the construction of lunar LLPs require that we adopt well known design procedures used on the Earth for slabs-on-ground. However, the adaptation of these methods to this case requires that information not available today be obtained to ensure a reliable design process. Information about the specific site selected for the construction to take place will be needed, including the appropriate range of values to use for the modulus of subgrade reaction to reflect the subsurface conditions. Due to friction, the LLP will also be restrained during thermal expansion/contraction. The extent to which the restraints will affect the strains in the LLP need to be considered, and thus the coefficient of friction will need to be quantified. As explained in our previous paper on the need for standard tests, dependable information is needed about the material properties and their variability before one can design with these materials [8]. And to know if the LLP can withstand the loads induced by a spacecraft, the mechanical durability of the materials to thermal loads and thermal cycles is needed. Chemical and radiation durability are also relevant information that is needed. Standard testing will be needed to verify the material properties of structural/mechanical materials made from Lunar regolith. Without experience in this extreme environment, engineers will be

even more dependent on testing materials to develop the data needed to design and build structures that meet the expectations. Brittle materials tend to be weak in tension and typically require the use of reinforcement to control cracking and add ductility. At this time, the use of such reinforcement is not expected to be an option. Note that certain empirical relationships used in this procedure will need to be verified, or updated, through experimentation, as mentioned in Section 2.4.

3. Data Characterizing Solicitations and Structural Properties

For the design of an LLP, as with any structural system, an engineer must consider two key aspects: (i) what hazards are relevant and what are the load (known as solicitations) and serviceability demands, and (ii) what probability of failure is acceptable. In this section we will address how we obtained the necessary design values used for the design of an LLP to be located at the Lunar South Pole based on a representative lander and candidate material. We define the material properties and conditions using the best available information.

3.1 Hazards

All expected loads and hazards should be identified and quantified at the location of the structure. Over its service life, an LLP will be subjected to numerous environmental and operational cycles. The Moon's environmental conditions include a large temperature range, radiation levels, micrometeorite impacts, moonquakes, and hard vacuum. A probable settlement location will be near the South Pole due to the likelihood of water in the form of ice [26]. The main environmental conditions to be considered are shown in Table 1.

Table 1. Environmental Loading Conditions for Lunar South Pole

Solicitation	Description
Temperature, °C	-71.15°C to -223.15°C in cycles of ~28 Earth days [27]
Gravity, m/sec^2	1.62
Radiation, mSv	380 [28]
Meteoroid Impacts	Particle sizes ranging from microns to centimeters Impact velocities ranging from 2.5 to 70 km/sec [29]
Seismicity, J/year	2.0×10^{10} to 2.0×10^{14} [30]

3.2 Loads

Loads will also be imposed on the LLP by vehicles and landers, primarily during launch and landing activities, which will introduce high temperatures and pressures. The mass of the spacecraft, the amount of thrust produced during launches and landings, and the potential impact force must be quantified for design. Several spacecraft have been designed by commercial companies, such as SpaceX's Starship and Blue Origin's Blue Moon. The landing mechanism design, such as number of legs, weight, weight distribution, and loaded area, affects the force that the LLP will experience during touchdown. Ideally, all legs would impact the pad at the same time, resulting in a concentric landing. However, cases of an imperfect landings may occur, resulting in a larger concentrated weight on fewer legs, or potentially even one leg coming first into contact. Thus, the LLP must be designed to withstand flexural and punching shear stresses, as explained in Section 2, caused by the impact force of the footpad(s). The relevant information that is available for potential landers is included in Table 2. The remainder of this paper will consider values associated with the Blue Moon to illustrate the approach and yield a design suitable for spacecraft up to 50 tons.

Table 2. Operational (Launch and Landing) Loading Conditions

	10 ton	Blue Moon (45 ton)	100 ton
Total Mass, kg	10,000	45,000	100,000
Maximum Vertical Plume Pressure, kPa [9]	25.0	39.6	42.9
Maximum Horizontal Shear Plume Pressure, kPa	0.25	1.13	2.50
Maximum Plume Heat Flux, kW/m^2	12,555.0	19,878.8	21,523.0
Maximum Surface Temperature, °C	Not reported	3,400	Not reported
Total Leg Force Applied, kN	16.2	72.9	162
Footpad Diameter, *estimated from images,* m	N/A	1.0	N/A
Vehicle Footprint Diameter, *estimated from images*, m	N/A	9.0	N/A

Static loads, such as the weight of the lander under lunar gravity, will affect the amount of deflection that the LLP will experience. The lander mass also influences long-term effects such as creep, where a sustained load causes increased deformation, or settlement, when the supporting soil allows the slab to move. It must be noted that time-dependent data used in the construction of the LLP, such as creep, fatigue, and temperature effects of the material, are important to establish life-cycle performance of an LLP. Additionally, after landing or before lift-off, the LLP may be subjected to additional loadings, such as transport vehicles driving across the surface or loading/unloading cargo. When these loads are significant, they can be considered by superimposing the deformations resulting from those loads on the deformations from those from the lander itself. Dynamic loads, such as acoustic and mechanical vibrations, may also occur.

The pad must be able to resist the lander's exhaust plume during landing and launching, which causes high temperature and pressure conditions (Table 2). During landing, the thrusters are often turned off to allow a short duration freefall. However, during lift-off the thrusters are at their closest point to the surface of the LLP, causing the most extreme temperature and pressure conditions. Plume considerations are discussed in Section 4.

The pad material must also be able to withstand the chemicals from the plume and potential fueling operations, as the propellants can contain liquid hydrogen, liquid methane, and liquid oxygen; the landing pad materials are unlikely to have been previously exposed to these chemicals on a regular basis. Durability to chemicals will require more information than is available now.

3.3 Structural Material Properties

Several construction methods have been proposed that would use regolith to manufacture construction materials in situ, including sintering, extrusion, and polymer infusion. Extruded or cast materials appear to be similar to concrete on Earth, but utilize in situ resources as replacements for ordinary concrete. For instance, molten sulfur has been proposed as a water replacement in the case of sulfur concrete, and aluminosilicate material has been proposed as a Portland cement replacement in the case of geopolymer concrete. Sintering of regolith can be achieved by solar, microwave, or laser energy and, at small-scale, exhibits behavior similar to that of a ceramic material.

Sintering involves compressing the raw material then heating at a temperature of 1000-1200°C,

which is just below the melting temperature of certain types of regolith [28]. A potentially important aspect of sintered regolith is that compacting the input material to decrease porosity appears to result in increased compressive strength [31]. Although the manufacturing process is energy intensive, sintered materials are viewed as promising candidates for full-scale ISRU construction. Additionally, among the materials being considered for Lunar construction, the literature does not have a complete set of material properties for design. For these reasons, the illustrative LLP example in Section 4 of this paper will adopt the properties for sintered regolith to illustrate the design approach and to discuss the relevant factors and trade-offs that will need to be made. However, the design procedure can be applied with any of these materials.

Table 3 provides the reported properties for two different heat-treated ISRU materials proposed for lunar construction: microwave sintered and laser vitreous material transformation. Properties of a ceramic material with a low coefficient of thermal expansion are also given, as this might be similar to sintered regolith. Note that due to the lack of standard test procedures and the limited size of the specimens that have been tested to date, these properties have been reported using inconsistent procedures, sample sizes, specimen dimensions, and testing conditions. It is likely that the true values will differ from these values. Before values for these material properties can be used in a final design, these properties must be tested using a consistent and reliable method at appropriate scale (the appropriate scale for such testing will also need to be determined) [8, 9, 10].

Table 3. Best Known Material Properties of Sintered Regolith [13]

Sintered Regolith Reported Material Properties	**Microwave Sintered**	**Laser VMX**	**Replicate Ceramic Material**
Compressive Strength, MPa (psi)	250 (36,259)	348 (50,473)	345 (50,038)
Tensile Strength, MPa (psi)	15 (2,176)	8.69 (1,260)	17.3 (2,509)
Modulus of Elasticity, GPa (ksi)	50 (7,252)	50 (7,252)	68.9 (9,993)
Coefficient of Thermal Expansion, 1/°C (1/°F)	$5x10^{-7}$ ($2.8x10^{-7}$)	$3.15x10^{-6}$ ($1.8x10^{-6}$)	$4x10^{-7}$ ($2.2x10^{-7}$)
Poisson's Ratio	0.25	0.25	0.25

3.4 Relevant Subsurface Details

Aside from the basic material properties of the LLP, the characteristics of the subsurface material must be known for design. Compacting the material under the landing pad will potentially be necessary for reducing settlement and increasing the maximum bearing capacity that the regolith can support. Uniform settlement occurs when the ground deforms downward at a constant rate under the applied loads. Differential settlement, which is when the ground deforms at different rates under the applied loads, may result from variations in the subgrade material or skewed loading and can cause cracking in the LLP. Limiting excessive differential settlement is especially important for LLPs since a tilted pad may prevent landings and launches, or complicate cargo offloading [2, 3]. Table 4 gives the reported properties of regolith simulants under a few relevant compaction levels. As noted in Section 2, the lack of data on actual levels of compaction and corresponding k that may be achieved on the surface of the Moon justifies the initial design be a stiff LLP.

Table 4. Relevant Regolith Properties [9, 13]

Regolith Properties	70% Relative Density	80% Relative Density	90% Relative Density
Density, g/cm^3 (lbm/ft^3)	1.56 (97.4)	1.64 (102.4)	1.77 (110.5)
Depth of Compaction, cm (in)	4.3 (1.7)	6.7 (2.6)	19.9 (7.8)
Modulus of Elasticity, MPa (psi)	20 (2,901)	22.5 (3,263)	25 (3,626)
Poisson's Ratio	0.23	0.25	0.27
Modulus of Subgrade Reaction, kPa/m (pci)	1,667 (6.1)	2,167 (8.0)	2,800 (10.3)
Cohesion, kPa (psi)	1.6 (0.23)	2.5 (0.36)	4.0 (0.58)
Friction Angle, degrees	44	48	52

The coefficient of friction between the compacted regolith and the material will also need to be determined to enable quantifying the strains due to restrained thermal contraction and the resulting tensile stresses. Typically, these stresses alone would be sufficient to crack the slab. Depending on the amount of friction that is present, these strains actually may be sufficient to cause cracking of the slab before the first landing.

3.5 Plume Response Considerations

The design of the LLP must consider the pressure and heat applied to the top surface of the LLP by the rocket plume during landings and launches. The rapid increase in surface temperatures, as well as the duration that the heating is applied, will influence the temperature and temperature gradients in the material on the inside of the LLP. Heating and cooling cycles will induce cracking (damage) wherever the strain is sufficiently high. Thus, both the subsurface conditions and the structural design (material, thickness, dimensions) selected to construct a given LLP will have a strong influence on the expected service life of that structure. The presence of damage (cracking) would likely result in the need for restrictions on the specific rockets that would be allowed to land on a given LLP of a certain design.

Because specific information about the plume temperature of each spacecraft is not available, we use an estimated temperature profile that is conservative as a worst case. Launch is going to introduce the more extreme thermal loads to the LLP, so a worst-case dynamic temperature profile launch scenario is developed. Mishra et al., [32] studied plume dynamics and gaseous plume interactions with the lunar soil. They estimated the translational plume temperatures based on hovering altitudes of the lander and the plume's corresponding radial distance. Worst-case launch temperature-time profiles based on [32] are used here, as shown in Fig. 7(a). For each radial distance, a corresponding maximum temperature is used. Temperatures are defined at radial distances of 0.7 m, 1.0 m, 1.3 m, and 1.7 m of 3400°C, 2100°C, 1200°C, and 800°C, respectively. The heating regime 1 (HR1) assumes that the lander is fully in contact with the LLP as the engines fire. This period lasts for a total of 1 minute and has the highest heating rate during the entire heating cycle. Heating regime 2 (HR2) assumes the lander has initiated launch and is no longer in contact with the LLP. In HR2 the heating rate is reduced compared to HR1, based on the assumption that there is no direct contact between the lander and the LLP.

Similarly, *Constant* and *Cooling* represent the constant and cooling regimes, respectively. The *Constant* phase assumes that the lander hovers at some distance from the LLP for some time before its full ascent. The *Cooling* regime assumes that the lander has ascended to the point where the plume no longer adds heat, and lowers the surface temperature to a nominal value. Here, a nominal (ambient) temperature of 20°C is used due to limitations of the software available for this analysis. Lunar surface

temperatures, however, range from -150°C and 150°C [32]. Based on first principles and considering the maximum surface temperature is 3400°C, the small offset in these temperature ranges is not expected to significantly affect the heat penetration into the LLP and is considered to be negligible. The LLP response to this temperature profile will be discussed in Section 4, followed by a discussion of results due to similar profiles.

4. Illustrative Design Example

Here we demonstrate the design of a square LLP using a first principles approach to determine the initial dimensions and to have a better handle on the safety factor. This approach is preferred to a finite element analysis to illustrate the impact of fundamental assumptions on the design outcome and the interactions of potentially competing objectives between LLP design choices. Due to the lack of information about the structural material, the allowable stress approach is adopted here to determine an initial thickness based on the expected service load. Subsequently, all of the other load cases will be considered. If any of the other load cases is not satisfied, the thickness will be adjusted and the process repeated. The input parameters used for design are summarized in Table 5. A plume analysis will then be performed to assess the damage, and the trade-offs to be made in the design of this type of structure are discussed at the end.

Table 5. Input Parameters Using Microwaved Sintered Regolith at 80% Relative Density

Parameter		Input Value
Mass of spacecraft, ton (kg)		50 ton (50,800)
Diameter of spacecraft, in (m)		354 (9)
Impact factor		1.3
a_s	Length of one side of pad, in (m)	1416 (35.97)
b_0	Critical shear perimeter, in (m)	153 (3.89)
D	Diameter of one footpad, in (m)	39.37 (1)
E	Modulus of elasticity, ksi (GPa)	7,252 (50)[2]
f'_c	Compressive strength of sintered regolith, psi (MPa)	36,259 (250)
k	Modulus of subgrade reaction, *assumed,* pci (kPa/m)	8 (2167)
μ	Coefficient of friction between slab and subgrade, *assumed*	1.5
ρ	Density of microwave sintered regolith, pcf (kg/cm^3)	162 (0.4)
ν	Poisson's ratio, *assumed*	0.25

4.1 Determination of Initial Thickness

Following the structural considerations described in detail in Section 2, the LLP will first be engineered to resist the impact of a 50-ton lander. The LLP is assumed to be built from sintered regolith and the design objective is to keep it uncracked under service loads. The lander characteristics and other assumptions used as inputs for the design process are summarized in Table 5. We design the LLP to have a dimension of three times the diameter of the spacecraft footprint, resulting in a 9 meter (354 in) outer dimension, making a_s = 1416 in (35.97 m) in Eq. (16).

An unplanned but likely critical scenario is assumed to perform the design, considering an uneven landing with initial touch down on one leg. The footpad diameter is 39.37 in (1 m). The lander load is increased by 30% to account for dynamic impact effects (a standard assumption for heavy trucks) [17]. Then, the initial thickness of the LLP is selected by limiting the critical tensile stress due to bending of

[2] A modulus of elasticity of 25 GPa was considered in the thermal analysis to allow for more flexibility and deformability in the pad, as explained in Section 3.5.

the pad resulting from a concentrated load due to the 50-ton lander. The critical stress is determined by considering each of the three conditions shown in Fig. 4. Equations (11) and (12) [Condition 1], (13) [Condition 2], and (14) [Condition 3] are used, and by rearranging Eq. (11), (13) and (14) we iteratively solve for the value of h (thickness) to keep the stress below the cracking strength of the LLP. An upper limit of 2/3 of the tensile strength for microwave sintered regolith (given in Table 3) of 15 MPa (2,176 psi) is set for f_t (allowable tensile stress). Of these three conditions, the critical case is found to be Condition 1 in which a single leg of the lander touches down at a corner of the LLP. The resulting initial thickness of the LLP for the 50-ton lander is 14 in.

To consider the more general case, Fig. 8 provides a plot showing the thickness required for the LLP obtained from the iterative solution of these equations. The controlling case for all thickness values considered here is Condition 1. For illustration, the thickness required to prevent flexural cracking for different sizes of landers is shown as a function of the tensile strength of the structural material. Three specific materials are then indicated based on best available information about their tensile strength. Note that an LLP made from microwave sintered material would need to be 14 in thick to withstand the landing case considered. If a material with a lower tensile strength were used, the pad would need to be thicker to withstand flexure.

The modulus of subgrade reaction also must be considered to account for the interaction between the pad and the subsurface. This study determines the level of compaction that would be required to support an LLP of a given thickness. Figure 9 shows that, with available information, the thickness of the LLP is relatively insensitive to the modulus of subgrade reaction for the range of values considered. Here the LLP is fairly rigid and will behave more like a rigid pavement than a flexible pavement. A rigid pad will distribute the load to the subgrade more uniformly over a wider area than a flexible pad would. This behavior would need to be reassessed if the material had a different tensile strength or if the LLP were considerably thinner.

4.2 Punching Shear

The punching shear strength for the initial 14 in thick LLP is next checked under the same concentrated load. A contact area that represents the 3 ft diameter, single-leg lander footpad is assumed. Like the case of bending tensile stresses, the diagonal tensile stresses that produce the truncated cone failure pattern in the case of punching shear must be maintained below the diagonal tensile strength of the unreinforced sintered regolith LLP. Equation (16) is used with the assumption that due to the lack of reinforcement, $V_{max}/V_{flex} = 1.0$. For the same reason, only 50% of the calculated strength will be used to check the thickness. Other modifications made to the approach reported in [23] are: (i) the effective depth is set to $d = 0.9(h)$, and (ii) as in reinforced concrete slab design, the expression of $4\sqrt{(f'_c)}$ will be used as the upper limit for the diagonal tensile strength in shear but using 36,259 psi as the compressive strength (f'_c) of sintered regolith from Table 3.

The critical shear perimeter ($b_0 = 2\pi r$) around the lander pad is defined by setting the critical radius equal to the radius of the footpad (1.5 ft), plus half of the effective depth, $d/2$. Thus, $b_0 = 2\pi(24.3$ in) = 153 in. The required shear strength is thus obtained from Eq. (16), and the available strength is calculated as $V_c = 4\sqrt{(f'_c)}\ b_0\ d = 4\sqrt{(36{,}259$ psi)(153 in)(0.9)(14 in) = 733,000 lb. Using only 50% of the strength, V_{max} = 366,000 lb is more than adequate to calculate the demand in Eq. (16) of 143,000 lb. Therefore, the initial thickness of 14 in is sufficient to resist punching shear without cracking.

4.3 Restrained Thermal Deformation

Next, a check of the tensile force and stress of the LLP is performed. The tensile force is due to a decrease in temperature that results in slab contraction. The contraction is resisted by frictional drag between the slab and the subgrade, causing a tensile force T. Using the best parameters available for microwave

sintered is still the assumed material, and T is found as 16,774 plf using Eq. (1). The values obtained as outputs of the LLP design process are provided in Table 6.

4.4 LLP Plume Response

Based on the calculated required thickness, a finite element model is developed to capture the heat penetration throughout the LLP, and to determine the mechanical strains that result from the constraints and thermal loads. This type of analysis is computationally intensive and the regions of the LLP that do not experience a thermal change or gradient are typically not included in the detailed model. Thus, an initial check is performed to determine what portion of the LLP would experience an increase in temperature due to the plume. Using a conservative load based on an extended 10-minute launch duration and a maximum temperature of 3400°C (Fig. 7(a)), we apply this thermal load over the 9 m diameter central region of the LLP. Due to the low heat conductivity of this material, the heat does not penetrate the lower 75% of the LLP, and does not spread radially much beyond the 9 m diameter of the lander. Large thermal gradients are however found to exist through the first 80 mm (3 in) of the LLP thickness.

Table 6. Output Parameters Using Microwaved Sintered Regolith at 80% Relative Density

Parameter		Output
h	LLP thickness, in (m)	14 (0.36)
T	Tensile force, lb per foot of slab width = plf (kN/m)	16,774 (248.71)
V_c	Available shear strength, lb (kN)	733,000 (3260.5)
V_{max}	Maximum shear strength from half the strength, lb (kN)	366,000 (1628.05)

4.4.1 Model

Because the extreme temperatures from the plume do not penetrate the entire LLP depth, only the portion of the LLP that is exposed to thermal changes and gradients must be modeled. The results will not change if the LLP section is larger than this region. Thus, we conservatively use an 18 m diameter circular section that is 0.177 m (6.9 in) deep. Due to the axisymmetric nature of the problem, a sliced section of the LLP is used for the model to save substantial computational time.

Utilizing the symmetry about the diametric plane, the half-sliced section, 9 m (354 in) long, 0.3 m (11.8 in) wide, and 0.177 m (6.9 in) deep is considered for the analysis. The sub-assembly considered in the model is depicted in Fig. 10. The 9 m-diameter central region is exposed to thermal loading with thermal loads applied at the top surface in accordance with the surface temperature boundary conditions shown in Fig 7(a).

The analysis is carried out using MASA, a general-purpose software developed at the University of Stuttgart [33, 35]. MASA employs temperature-dependent micro-plane models for quasi-brittle materials such as concrete. To develop the finite element mesh, 8-noded hexahedral elements with 8 integration points are used, with 15 mm cubic elements. The use of a coarse mesh (>15 mm) would average the mechanical strains across larger element sizes, affecting the precision of the strain behavior for a thermally-loaded section. On the other hand, an even finer mesh is computationally expensive and does not substantially improve the accuracy of the results. Thus, 15 mm is selected for improved accuracy in the damage (cracking) volume determined with the model and for adequate visualization of the strains. Note that the software utilized in this work utilizes a smeared crack approach, where the cracks are represented as average strains smeared over the element [34]. This approach is adopted due to is computational efficiency and ease of modeling. The analysis captures the overall behavior and crack pattern well, which is useful for practical design and analysis. More intricate analysis following the discrete crack approach and more refined models is out of scope of this paper.

Symmetric boundary conditions are added in the *y*-plane based on the symmetry at the diametric plane of a full-sized model, as depicted in Fig. 10. Constraints are applied in the *x*- and *z*-directions, as shown in Fig. 11. Fixed boundary conditions in the *x*-direction are implemented along the sides of the sliced section to account for the stresses imposed by the surrounding LLP material due to thermal expansion.

The modulus of subgrade reaction will introduce compliance below the LLP. Compliance is helpful here to mitigate cracking in the LLP, although considerations must be made to minimize settling. To model the elasticity of the subsurface, a series of compression-only springs (shown in red and yellow), known as a compression bar, is used to account for the subgrade reaction modulus. Without some compliance introduced in the subsurface, the LLP was found to experience cracking throughout its thickness in all thermal loading scenarios.

For illustrative purposes, the nominal material properties shown in Table 3 are modified. Specifically for this analysis, we consider a modulus of elasticity of both 50 GPa (nominal) and 25 GPa (modified). The modified material has corresponding compressive and tensile strengths of 250 and 30 MPa, respectively. As already mentioned, cracking is expected with these brittle materials, and reliable values for these parameters that correspond to the manufactured materials at scale are not yet available. Thus, we assume reasonable values that, based on experience, may also be able to resist the high tensile stresses that are produced by the thermal loads. More flexibility and deformability are needed in the LLP to prevent it from cracking. In the discussion in Section 5 we will explain how these values interact with the requirements for mechanical loading to influence the design. Note that the authors used the values of thermal properties from the literature that are determined for the Earth's environment. For a more realistic assessment, the thermal properties should be determined compatible with the lunar environment.

Thermal loads are applied to the inner 4.5 m of the sliced LLP by setting temperature boundary conditions for the relevant nodes and elements at the top surface of the LLP (Fig. 11). Temperature and heat flux boundary conditions for the nodes and elements located on the top surface of the LLP are added, respectively. Several different runs are performed with different durations and different ultimate temperatures based on the plume heating profiles in Fig. 7(a,b).

4.4.2 Results

Fig. 12 presents the internal temperature at a depth of both 25 mm and 50 mm for each of the load cases using the conservative 10 min temperature profile. Note that for all thermal load cases, by five minutes into the temperature profile, there is a noticeable jump in the internal temperature. This jump is attributed to the rather low thermal conductivity of the LLP material. Note that in Fig. 7(a), plume temperatures reach their maximum in HR2 and remain there until the end of the Constant phase at five minutes. Only when the plume cycle reaches the Cooling regime do the temperatures decrease.

Due to the short heating cycle and massive heating rates in the first and second heating regimes, the LLP experiences significant temperature gradients, with high temperatures at the surface but low penetration into the structure. This behavior is due to the low thermal conductivity of the material. As the lander ascends, the heat penetrates into the thickness of the LLP even after the temperature begins to drop at the surface. This behavior is analogous to that observed in concrete exposed to fire. The temperatures within the concrete continue to rise even after the fire exposure ends [36]. During the cooling phase, a rapid decrease in internal temperature occurs due to the decrease in the surface temperature. Thus, there is a short duration of the high temperature exposure to the LLP material. Once the respective depths have experienced the full heating cycle, both surface temperatures and internal temperatures decrease to ambient.

Recall that the sliced section has fixed boundary conditions in the *x*- and *z*-directions due to the axisymmetric nature of the problem. With these boundary conditions, the model does not allow for any heat to escape through the sides of the pad, thus mitigating the likelihood of any radiative cooling from

the sides of the LLP (Fig. 10). This behavior is representative of a full-scale LLP since the LLP will be considerably larger than the region exposed to the plume. This localized loading hinders the radiative cooling from the sides due to the considerable distance needed for the heat to propagate laterally to reach the curved exterior surface of the pad.

Due to the low heat conductivity of the material, the depth of the LLP sliced section, and the duration of plume exposure, convection into the regolith below the LLP is negligible. Although the assumed plume cycle (Fig. 7a) is already quite conservative in terms of the duration of exposure, the heat does not fully penetrate through the depth of the LLP. In Fig. 12, even in the worst thermal loading case (*i.e.*, 3400°C), a substantial internal temperature drop is obtained at 50 mm of depth (black dotted line) in comparison to that at 25 mm (black solid line). Temperatures at the bottom surface of the LLP remain ambient, which is attributed to the low thermal conductivity of the material and short exposure duration. Notably, the duration of exposure also represents a highly conservative case of thermal exposure onto the LLP. In a realistic scenario, the plume exposure would be much shorter, which would greatly reduce the likelihood of convection into the regolith.

Damage in the LLP due to the thermal loading is realized as cracking. Cracking is common in brittle materials that are in service on Earth. Here, a smeared crack approach is used to capture the cracking [33, 37] and a maximum mechanical strain of 0.02 is used. Thus, red colored contours correspond to a principle tensile strain of more than or equal to 0.02, which for the element size of 15 mm corresponds to a crack width of 0.3mm or greater in context of the smeared crack approach. The choice of 0.3 mm crack width is arbitrary to some extent and is taken here to display the damage to the LLP visually. However, this crack width corresponds to the generally accepted crack width limit for serviceability limit state of concrete structures.

Each of the following load cases seen in Fig. 13 and Fig. 14 represents the strain experienced after each phase in the plume heating cycle. For instance, in a typical reinforced concrete member, a minimum allowable crack width is imposed for serviceability purposes [38]. The typical allowable crack width is 0.3 mm for structural reinforced concrete members. As a result, the strains seen correspond to a 0.3 mm crack width for a standard size concrete crack within the framework of crack band method [39]. Although these refer to a standard size serviceability crack, this value is subject to change based on definitive lunar conditions. Thus, a maximum strain of 0.02 is represented as the maximum damage, shown in red in Fig. 13 and Fig. 14 (element size = 15 mm). Fig. 13 and Fig. 14 represent the strains experienced by a sliced section of the pad between the thermally loaded and non-loaded end of the pad at each end of the phase.

As shown in Fig. 14, with a maximum strain of 0.02, the 800°C load case experiences only a maximum of 0.008 strain, whereas the 1200°C case experiences a maximum 0.02 strain at the end of the cooling phase. In addition, the 1200°C load cases experience maximum damage (0.02 strain) at the end of the cooling phase. Although the results are representative of a single landing, it is important to note that the first landing is expected to represent the greatest damage or cracking within the LLP. With microcracks already present on and throughout the pad after the first landing, the rate of damage to the LLP is expected to decrease with subsequent landings. This behavior is attributed to the relief of localized stresses due to the presence of existing microcracks from previous landings, thus reducing the likelihood of additional crack formation.

Fig. 14 represents mechanical strains seen for higher plume temperatures of 2100°C and 3400°C, respectively. In both cases, maximum strains can be seen at the end of the cooling phase for both thermally loaded cases. However, maximum damage is seen within the first heating regime for maximum temperature exposure: 3400°C in comparison to the 2100°C case.

Although a conservative temperature profile is assumed as a worst-case scenario, we also considered some cases with a 60 and 100 sec duration launch, using the same shape shown in Fig. 7 to illustrate that cracking will still be likely. The mechanical strains seen within Fig. 15 are representative

of the results due to plume exposures of 100 sec and 60 sec, respectively. From these two cases, it is seen that both exposures do not yield the maximum damage (allowable cracking) beyond a 15 mm depth (0.6 in) at the end of the cooling phase.

In all thermal load cases, the maximum damage, as depicted by a 0.02 mechanical strain, occurs in the LLP when undergoing the cooling phase as well as when the cooling phase ends. This result is due to the thermal expansion and contraction that occur due to high thermal gradients. The end of the cooling phase indicates that at 10 minutes of the heating cycle, surface temperatures are cooling to ambient temperatures. However, internal temperatures remain high, as can be seen in Fig. 12. Thus, tensile stresses occur due to the internal LLP core wanting to expand, while the surface starts to shrink due to cooling. This behavior induces the maximum strains that are seen at the end of the cooling phase. Although there is clear damage within the first 50 mm of the depth of the section, no maximum strain is seen near the bottom surface of the pad with the maximum temperature exposure (3400°C).

The high heating rate combined with low thermal conductivity of the LLP material is expected to result in large thermal gradients and thermal stresses. The actual state of thermal gradients, stresses, and damage depends on many factors such as the structural properties of the material, thermal properties of the material, geometry of the LLP and boundary conditions, as well as the temporal and special temperature profiles due to the plume. The assumptions made in this paper are realistic, but can vary significantly based on the design and the material considered.

Note that repeated thermal and mechanical loading is likely to further exacerbate the damage and should be accounted for through appropriate safety margins. However, it is important to remember that in subsequent landings, the same amount of damage is not expected after the first landing due to the existing microcracks, which leads to the relief of localized stresses, inducing less crack formation for future landings.

5. Discussion

Establishing a robust Lunar economy will require infrastructure to facilitate consistent safe delivery of crew and consumables to the Lunar surface. An LLP will be one of the first infrastructure elements that, due to its size and expected demands, will be best accomplished using ISRU-based structural materials. Meeting this objective on a reasonable timeline will require that we prioritize collecting the information that is most critical for starting with a safe and useful structure, knowing that it will have a limited service life, and then learn as much as possible from observations and data collection during the construction and operation of that structure under a variety of service conditions. Later, a long-term facility for structural and durability testing of these materials will need to be established on the Moon to develop the knowledge needed to build more complex structures from these classes of materials.

This paper is focused on the design of such a reusable LLP made from ISRU-based structural materials. The process of structural design is a complex problem that involves structural analysis, material selection, load calculations, adherence to codes and standards of practice, and consideration of factors like stability, strength, and serviceability, all focused on achieving a safe and performant, yet cost-effective and often aesthetically pleasing outcome. In extending the structural design process to the extraterrestrial environment, several special considerations are deemed worth discussing further as we conclude this paper as they can have significant impact on the safety, durability and feasibility of LLPs.

When facing the design of a structure that falls outside the range of standard practice, a return to first principles is essential. Design that falls outside of standard practice can refer to materials that we do not understand yet, or loadings that we cannot characterize yet, or environmental conditions that we do not yet have experience with. Past experience designing LLPs and airport runways on the Earth support the development of the design approach presented in this paper. Limitations on the range of available materials and their properties, as well as the uncertainty in the knowledge of the soil properties which will serve as the base and subbase for the LLP, further complicate the design. Furthermore, in the

absence of prescriptive codes and standards for both materials and design of LLPs in extraterrestrial conditions support the selection of a performance-based design, and this approach is adopted herein.

Clearly the first LLP built on the Moon will need to be designed to survive and meet the operational needs associated with regular launches and landings for a period of time. We recommend that a robust build-observe-test-learn approach be implemented to gain the experience needed to build infrastructure in extraterrestrial environments, starting with the lunar surface. Note that the type of finite element models discussed herein and those considered by other researchers may be suitable for examining macroscopic behavior but are not appropriate for the prediction of microstructure behavior. Such models have a limited ability to predict crack propagation, especially in brittle materials. Finite element models will also be useful for considering more complex scenarios to refining the design process, or for exploring localized design features that may serve to control cracking in specific regions. For this, design basis scenarios considering the regular operation loads (regular landing and launching), anticipated occupational occurrences (such as unsymmetric landing) and accidental scenarios (landing close to the edge, higher plume pressure or impact velocity) should be determined. Testing is required to develop experience with the materials. Ductility is added to brittle materials through the addition of reinforcement to control cracking, as is done in concrete on Earth. Confinement is another way to control cracking by inducing an active stress state to the material. Neither of these options that are ubiquitous in structural engineering on Earth seems to be compatible with the types of methods that are being proposed for construction on the Moon at this time.

Serious gaps in knowledge still exist that will hinder the design of safe and reliable reusable LLPs for the Moon, or any extraterrestrial body. First and foremost is the geotechnical characterization of the ground supporting the LLP. Given the expected size of an LLP, tens of meters in diameter, and the significant loads it will have to withstand, including its self-weight, it is absolutely necessary to have sufficient information of the natural soils under the LLP, over the depth of influence of the structure; that is, over tens of meters of depth. The information required includes the geotechnical description and characterization of these soils and/or rock underneath as well as their mechanical properties, which may be time- and load-dependent (including temperature). It will also be important to characterize the soils that will lie directly underneath the slab. Those could be either the soils found at the site, if deemed appropriate to adequately support the expected loads with tolerable deformations, or soils that may be transported from another site to serve in this capacity. It will be necessary to understand how to effectively compact these materials in situ and what mechanical properties can be achieved with different degrees of compaction. The rocket plume may also induce vibrations that will affect settlement and compaction. While all of this information is quite relevant to be able to achieve the needed levels of compaction at sufficient depth to serve as sound support for the LLP, what level of compaction will be needed remains an open question. To deal with the vast uncertainties associated with the behavior of the ground, we recommend an approach to design that maintains the LLP uncracked and increases its stiffness thus decreasing its sensitivity to the modulus of subgrade reaction.

One of the driving loading scenarios to be considered for the design of LLP is the cycles of temperature rise and fall due to the rocket plume. The heating rate, highest temperature, lowest temperature, cooling rate, temperature exposure duration, and repeated heating/cooling cycles (due to repeated landings and take-offs), are all highly relevant and important parameters that can influence the effect of plume exposure on the LLP. Combined with material properties such as thermal conductivity, heat capacity, modulus of elasticity, tensile strength, etc. as well as the boundary conditions and soil conditions can have a strong influence on the temperature gradients, thermal stresses and the damage caused to the LLP. Currently, we know little about these properties and have to assume several parameters based on past experience and engineering judgement. Even where we use certain estimates of material properties such as compressive or tensile strength, those values are typically obtained from very small-scale specimens and their applicability on realistic structural scales is largely unknown.

Note that our analysis considers a variety of scenarios, some of which are typical operational scenarios and some are accident or worst-case scenarios. The plume analysis considers extraordinarily long temperature profiles that might occur when a spacecraft has an emergency. The duration of the high-temperature period and the presence of any restraint to this structure under thermal loads seem to be especially influential on the amount of cracking that is predicted in such a brittle material. Internal cracking within the LLP is certainly damage, but that type of damage is similar to a reduction in the elastic modulus of the material and may actually add some flexibility to the structure and relax the stress state. Surface cracking is the critical case, as some studies have shown that debris on the pad during a launch or landing are likely to achieve escape velocity and reach orbit [11].

Clearly, the regolith properties used herein, while the best available at this time and reasonably adequate for illustrating the design and analysis processes, should not be used for design. Those properties should be obtained, as it is done on Earth, from in-situ exploration and testing. Initially, the approaches and techniques used on Earth could be used on the Moon, but acknowledging the limitations due to the completely different environment. The subsurface stratigraphy and depth of rock could be established from geophysical methods. For example, seismic testing could provide the shear wave velocity profile with depth, which could be used to estimate the different layers, if any, below the surface, as well as the depth of the regolith to rock. The shear wave velocity would also provide information about the small-strain stiffness of the different materials at depth, which then can be used as input into more representative soil models that account for changes in regolith stiffness with confinement and with shear. To estimate the strength of the soil/regolith deposits at the LLP site, more intrusive testing will be necessary. On Earth, those take the form of CPT (cone penetration tests), where a calibrated cone is pushed into the soil at a pre-determined rate, while the tip and shaft/sleeve friction forces are measured. Those forces are then used, through calibrations and empirical correlations to determine the type of soil, internal friction angle of the soil, coefficient of earth pressure at rest, relative density, etc. Again, while those estimates could be used, it has to be realized that they have been obtained empirically under Earth's gravity and, thus, may not be applicable to other environments where the gravity is much different than that of the Earth. All this strongly suggests that a test laboratory should be established on the Moon, where materials and probes can be tested with the Moon's environment.

To minimize some of these uncertainties, the first slab to be designed could be designed to reduce the impact of the unknown support quality of the native soil as previously noted. In addition, knowledge of the coefficient of friction between pad and ground will be important to control cracking of the LLP due to restrained thermal movements. Without testing standards to properly ascertain the reliability of the properties, an allowable stress design is deemed the most appropriate design strategy to achieve an adequate factor of safety. Clearly, the larger the uncertainties, the more conservative the design should be. This consideration, of course, raises the cost and the time of construction. Then, in situ testing and observation should exploit that structure under many types of loading conditions. The build-observe-test-learn approach that we are recommending for the first LLP should be preceded by acquiring the highest priority data from testing done in situ through CLPS missions, and it would be followed by the establishment of an in situ testing facility for structural materials to address the questions that remain and gain an understanding of the conditions, materials, variability and uncertainties that will lead to future safe and reliable designs.

There are several open questions and variables that must be known with reasonable certainty for the analysis to be realistic and reliable. In the absence of more information, this paper leverages the vast information available based on experience with similar materials and systems on Earth. The basic assumption made on the mechanical behavior of the material of LLP is that it is a quasi-brittle material with a relatively high ratio between its compressive and tensile strength, similar to that observed for concrete on Earth. The material as well as thermal properties are assumed based on the data available for two different heat-treated ISRU materials proposed for lunar construction: microwave sintered and

laser vitreous material transformation. Although the exact values of the material properties might vary, the general outcomes and conclusions are not expected to drastically change from the ones obtained using the assumed properties.

Scientists, researchers, and engineers need to come together with the most important challenges that will drive the design and how to solve them to achieve a realistic and realizable design of LLP. One of the highest priorities should be assigned to understanding the material behavior at scale. Testing very small sizes may result in ambiguous or unrealistic results due to size and scale effects [8]. A representative size and shape of the test specimen as well as standardized methods of testing and correlating the results to the properties expected at scale are extremely important to attempt for structurally safe and sound designs. Understanding material performance under lunar conditions is another highly important aspect, for which equipment such as thermal-vacuum chambers can provide solutions in terms of the balance of economic considerations and realistic testing, here on Earth. Assessing the variability in material properties would be needed for estimating the reliability of the LLP, but can be taken up after the basic material behavior and performance at scale and under lunar conditions are established.

To consider an appropriate path forward it may be useful to classify the above activities into short-, medium-, and long-term steps. We define these as follows: short-term refers to activities that should take place before the first LLP is constructed; medium-term relates to observations and experiments that take place while operating the first LLP, especially in the firsts several years; and long-term refers to the period beyond that that involves both observations related to durability over their service life and using that information to construct additional LLPs (and other structures) from these indigenous materials.

In the short term, it will be necessary to collect all available information about the potential site: topography, surface materials (regolith, rock), etc. The materials to be used should be characterized, at scale, to obtain their properties. The appropriate size of the specimens to get representative behavior will need to be determined [8]. Planned missions to the surface of the Moon should be exploited to gather information through testing to obtain information such as the in-situ shear wave velocity profile, seismicity at the potential site. It is possible that, because the landing pad is not built yet, the tools and instruments available will be very limited. So, limited insight into the subsurface ground conditions may be achieved. During these missions, in situ testing of the materials for strength and thermal effects should also be conducted, in parallel with as realistic as possible testing under these conditions on Earth, as well as efforts to obtain the coefficient of friction at the site between the regolith and the material that the pad will be made of, to inform the design. During the construction and any exploration done prior to construction it would be best to update the site geology and ground properties at the site. The site should be instrumented and monitored during construction to learn about ground behavior under lunar conditions, especially lunar gravity.

In the medium term, the LLP will be operational, and will serve as a testbed. The LLP should be instrumented to capture settlements, strains and temperature, and cracking should be captured visually. It will be important to capture the loads imposed during each landing and launch, including both the force history associated with the landing impact and the plume temperature, duration and pressure. Assumptions made for the design of the pad should be verified through observations and data collection. Interactions between the pad and the subsurface can be observed during thermal cycles and thermal and mechanical loadings. With the LLP operating and the access it provides to deliver cargo to the Moon, a facility for structural and durability testing of these materials should be established on the Moon to build the knowledge needed to construct the next structures from these classes of materials. Having this facility and examining the variability in the material properties of the manufactured regolith would also directly support the establishment of standards to enable further construction using those, and other classes of, suitable materials.

In the long term, after the first several landings, the data to be gathered using the subsurface, embedded and surface instrumentation can be used to consider durability and performance. Radiation, chemical spills, landing and launches that cause cracking, and exposure to the lunar conditions are all potential sources of long term degradation. Each landing and launch should be used as an opportunity to collect data. The availability of more accurate definition of the subsurface conditions, collected during construction and the first few landings and launches, will allow for a better understanding of the long term performance of the LLP. Exposure to the lunar environment is expected to inform durability models, and test maintenance actions in the field. During this period, in-depth site exploration should be done, and it may also be possible to learn about effects of extreme events such as seismicity and meteoroid impact.

As mentioned previously, the landing pad design will need to be consistent/commensurate with the information known about the material, behavior, site and loads. The initial design should be based on existing tools and properties taken from analogous sites/soils on Earth. Note that if the LLP needs to be reusable, the design of the first structure will need to be conservative. Over time, design procedures should be refined to better construct all future structures and to maintain the initial LLP.

6. Conclusions

Although it is clear that there are currently many unknowns and gaps in knowledge related to the construction of ISRU-based structures, this challenge is not new in the field of civil and structural engineering. Civil engineering certainly has the expertise and ability to safely build structures that perform under the most extreme conditions given the availability of data and standards to ensure that material performs repeatably and reliably. The native materials that have been studied and used for construction over decades on Earth also have large variability in their properties. Additionally, design loads must often be estimated and the models used are quite idealized and inaccurate in many cases. Still, civil and structural engineers will be able to create safe and reliable structures under these conditions. Furthermore, these challenges must not all be resolved at once; they can be addressed based on priority.

The construction of the first LLP is not going to be preceded by large quantities of in situ testing that will confirm that it is being constructed properly for the activity that is expected. However, it will still need to be built to operate and survive until another, resilient LLP is operational. Building that structure, making detailed observations, taking thorough data, and learning from all of those procedures will be the way to generate important lessons on how all of this will be done better. The expectations and vulnerabilities of that system will also become clearer over time. To ease this process, space science activities should prioritize the collection of these data to help realize safer and more reliable structures.

Infrastructure such as LLPs, roadways, and habitats will be essential for upcoming lunar exploration missions. However, before an engineer can design these structures, additional data must be obtained to quantify site conditions, loading, and material properties for ISRU construction. Until reliable data is collected in situ, designers interested in the sensitivity of the design and dimensions to material properties and site conditions would be able to implement this design approach while varying the parameters. This approach would also allow for a study on the design using different materials and its impact on design, and assessment of the relevant resource needs and costs. The build-test-use-learn approach we propose will evolve our knowledge and lead to a refined understanding of what is possible with these structural materials. In time, a testing facility will be needed on the Moon to perform soil studies, structural testing, and durability investigations for any of the materials that may be used for support or for manufactured materials for structures. This facility would have the correct gravity, which is critical for soil properties. Furthermore, it would be possible to realize the proper environmental conditions without the need for thermal vacuum chambers. The capability to perform repair and

maintenance actions may also be examined. Until that time, we will need to leverage the vast amount of experience accumulated in civil engineering and collect as much data as possible about the conditions, loadings and expectations for these structures.

7. Declaration of competing interest

The authors declare that they have no known competing financial interests or personal relationships that could have appeared to influence the work reported in this paper.

8. Acknowledgement

This material is based upon work performed in part through the Resilient Extra-Terrestrial Habitat Institute (RETHi) supported by a Space Technology Research Institutes grant (number 80NSSC19K1076) from NASA's Space Technology Research Grants Program.

9. References

1. U.S. Department of State, *Memorandum on Space Policy Directive 7,* Presidential Memoranda, White House, Washington, D.C., 2021 https://trumpwhitehouse.archives.gov/presidential-actions/memorandum-space-policy-directive-7/
2. Mueller, R. P. "Lunar Landing & Launch Pads," Lunar Surface Innovation Consortium Excavation and Construction Focus Group https://ntrs.nasa.gov/api/citations/20205009125/downloads/Lunar%20Landing%20%26%20Launch%20Pads%20v1.pdf
3. National Aeronautics and Space Administration, Lunar Surface Cargo, Moon to Mars Program, 2024. https://www.nasa.gov/moontomarsarchitecture-whitepapers/
4. National Aeronautics and Space Administration, Lunar Logistics Drivers and Needs, Moon to Mars Program, 2023. https://ntrs.nasa.gov/citations/20230016304
5. National Aeronautics and Space Administration, Safe and Precise Landing at Lunar Sites, Moon to Mars Program, 2023. https://ntrs.nasa.gov/citations/2023006301
6. Skidmore Owings and Merrill, Accessed May 12, 2025. https://www.som.com/projects/burj-khalifa/
7. American Concrete Institute (ACI), *Ultra-High-Performance Concrete: An Emerging Technology Report*, ACI Committee 239 Report, 2018, 21 pages, ISBN: 978-1-64195-034-3.
8. Dyke, S.J., Sharma, A., Mount, E.M., Bobet, A., Ramirez, J.A. "Establishing Standards for Lunar ISRU Structural Materials," AIAA Journal, Vol. 62, No. 7, 2024, pp. 2414-2423 https://doi.org/10.2514/1.J063816
9. Jehn, I.E., Dreyer, C.B. "A Design Methodology for Flat Slab Lunar Landing and Launch Pad Systems," *Acta Astronautica*, Vol. 231, pp. 175-192, 2025 https://doi.org/10.1016/j.actaastro.2025.02.046.
10. Bazant, Z.P. and Planas, J. (1998). *Fracture and Size Effect in Concrete and Other Quasibrittle Materials*. CRC Press, Boca Raton, FL.
11. Metzger and Mantovani. "The Damage to Lunar Orbiting Spacecraft Caused by the Ejecta of Lunar Landers," Proceedings of the ASCE Earth and Space, 2021, pp. 136-145. doi:10.1061/9780784483374.014
12. Metzger, P.T., Autry, G.W. "The Cost of Lunar Landing Pads with a Trade Study of Construction Methods," Mary Ann Liebert, Inc. Publishers, Vol. 11, No. 2, 2023. https://doi.org/10.1089/space.2022.0015

13. MMPACT Project, *ICON Project Olympus Presentation*, LSIC Spring Meeting https://www.darpa.mil/sites/default/files/attachment/2024-12/icon-luna-10.pdf
14. American Association of State Highway and Transportation Officials (AASHTO). *LRFD Bridge Design Specifications*, 9th Edition, Washington, DC, 2020. ISBN: 978-1-56051-738-2
15. Losberg, A., "Pavements and Slabs on Grade with Structural Active Reinforcement," *Journal of the American Concrete Institute*, Vol. 75, No. 12, 1978, pp. 647-657. DOI: 10.14359/10977
16. Post-Tensioning Institute (PTI). *Design and Construction of Post-Tensioned Slabs-on-Ground*, Farmington Hills, MI, 3rd ed., 2004, 2008 Supplement, pp. 155.
17. American Association of State Highway and Transportation Officials (AASHTO), 1993. *Guide for Design of Pavement Structures*, Washington, DC: American Association of State Highway and Transportation Officials, II-45
18. Westergaard, H.M. *Stresses in Concrete Pavements Computed by Theoretical Analysis Public Roads*, Federal Highway Administration, Vol. 7, No. 2, 1926, pp. 25-35.
19. Westergaard, H.M. *Analysis of Stresses in Concrete Roads Caused by Variations in Temperature Public Roads*, Federal Highway Administration, Vol. 8, No. 3, 1927, pp. 201-215.
20. ASTM D1196/D1196M-21 Subcommittee E17.41, *Standard Test Method for Nonrepetitive Static Plate Load Tests of Soils and Flexible Pavement Components, for Use in Evaluation and Design of Airport and Highway Pavements*, ASTM International, Vol. 04.03, 2024, pp. 1-10. DOI: 10.1520/D1196_D1196M-21
21. American Concrete Institute Committee 360*, Guide to Design of Slabs-on-Ground*, Farmington Hills, MI, 2014, pp. 77. ISBN: 9780870313714 (2010)
22. Portland Cement Association (PCA)*. Design of Heavy Industrial Concrete Pavements*, IS234.01P, Skokie, IL, 1988, pp. 12.
23. Moe, J. *Shearing Strength of Reinforced Concrete Slabs and Footings under Concentrated Loads*, Development Department Bulletin D47, Portland Cement Association, Skokie, IL., 1961
24. ACI-ASCE Committee 326*. "*Shear and Diagonal Tension Slabs," *ACI Journal*, Vol. 59, No. 3, 1962, pp. 353–396.
25. ACI Committee 318, 2025. *Building Code Requirements for Structural Concrete (ACI 318-25) and Commentary (ACI 318R-25)*, American Concrete Institute, Farmington Hills, MI. https://www.concrete.org
26. Zuniga, A., Turner, M., Rasky, D., Loucks, M., Carrico, J., Policastri, L. "Building an Economical and Sustainable Lunar Infrastructure to Enable Human Lunar Missions," *Proceedings of the AIAA Space and Astronautics Forum and Exposition*, September 12-14, 2017, Orlando, FL. https://doi.org/10.2514/6.2017-5148
27. Williams, J.P., Paige, D.A., Greenhagen, B.T., Sefton-Nash, E. "The global surface temperatures of the Moon as measured by the Diviner Lunar Radiometer Experiment," *Icarus*, Vol. 283, 2017, pp. 300-325. https://doi.org/10.1029/2019JE006028
28. Naser, M.Z., "Extraterrestrial Construction Materials*," Progress in Materials Science Journal*, Vol. 105, 2019, Article 100577. https://doi.org/10.1016/j.pmatsci.2019.100577
29. Moorhead, A.V., Koehler, H.M., Cooke, W.J. *NASA Meteoroid Engineering Model Release 2.0* National Aeronautics and Space Administration Technical Reports Server (NTRS), NASA/TM-2015-218214, 2015. https://ntrs.nasa.gov/citations/20150021449
30. Heiken, G.H., Vaniman, D.T., French, B.M. *Lunar Sourcebook: A User's Guide to the Moon*, Cambridge University Press, 1991, pp. 27-60 https://www.lpi.usra.edu/publications/books/lunar_sourcebook/pdf/LunarSourceBook.pdf

31. Indyk, S.J., Benaroya, H. "A Structural Assessment of Unrefined Sintered Lunar Regolith Simulant," *Acta Astronautica,* Vol. 140, 2017, pp. 517-536. https://doi.org/10.1016/j.actaastro.2017.09.018
32. Mishra, S. K., Prasad, K. D., Nath, P., Agarwal, D., Kumar, S. S., & Bhardwaj, A. (2021). "Effect of Lunar Landing on its Surface, Surrounding Environment and Hardware: A Numerical Perspective," *Planetary and Space Science*, 211, 105398. https://doi.org/10.1016/j.pss.2021.105398
33. Ožbolt, J., Li, Y., and Kožar, I. "Microplane model for concrete with relaxed kinematic constraint," *International Journal of Solids and Structures*, 38(16), 2001. 2683–2711. https://doi.org/10.1016/s0020-7683(00)00177-3
34. Bazant and Oh, 1983. "Finite Element Modeling of Crack Band Propagation," *Journal of Structural Engineering*, American Society of Civil Engineers, Vol. 109, No. 1, pp. 69. https://doi.org/10.1061/(ASCE)0733-9445(1983)109:1(69).
35. Ožbolt, J., Bošnjak, J., Periškić, G., and Sharma, A. "3D Numerical Analysis of Reinforced Concrete Beams exposed to elevated temperature," *Engineering Structures*, 58, 2013, pp. 166–174. https://doi.org/10.1016/j.engstruct.2012.11.030
36. Das A, Bosnjak J, Sharma A., "Post-fire Bond Behaviour of Reinforcement in Concrete Considering Different Bonded Lengths and Position of Rebars," *Engineering Structures,* 296 (2023) 116908
37. Ožbolt, J., Bošnjak, J., Periškić, G., & Sharma, A. (2013). 3D numerical analysis of reinforced concrete beams exposed to elevated temperature. *Engineering Structures*, *58*, 166–174. https://doi.org/10.1016/j.engstruct.2012.11.030
38. FIB. (2013). *Fib Model Code for Concrete Structures* 2013. Ernst & Sohn, Wiley. Ghent University Academic Bibliography.
39. Bažant, Z. P., & Oh, B. H. "Crack Band Theory for Fracture of Concrete," *Matériaux et Constructions*, 16(3), 1983, 155–177. https://doi.org/10.1007/bf02486267
40. Wight, J. K. *Reinforced Concrete: Mechanics and Design*, Pearson, 8th ed., 2022.

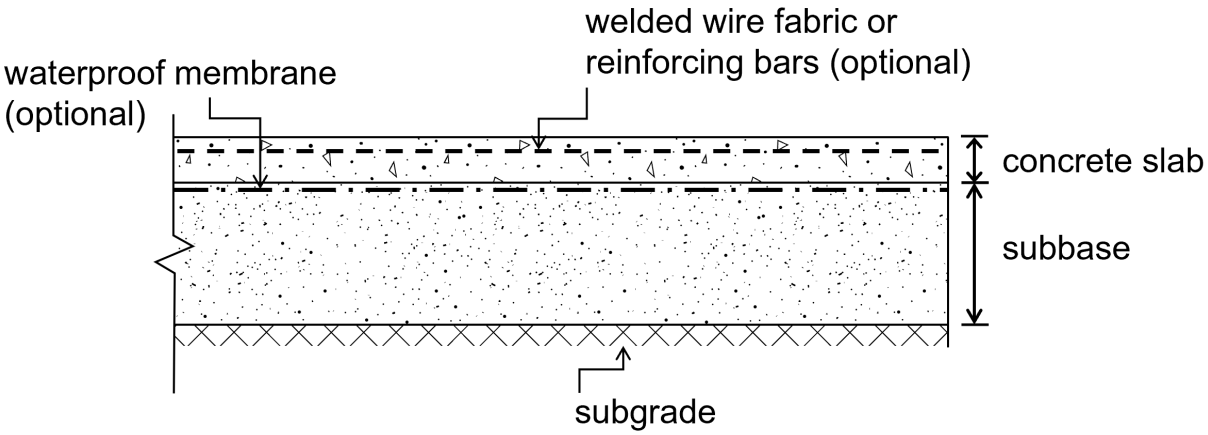

Fig. 1 Typical slab-on-grade construction

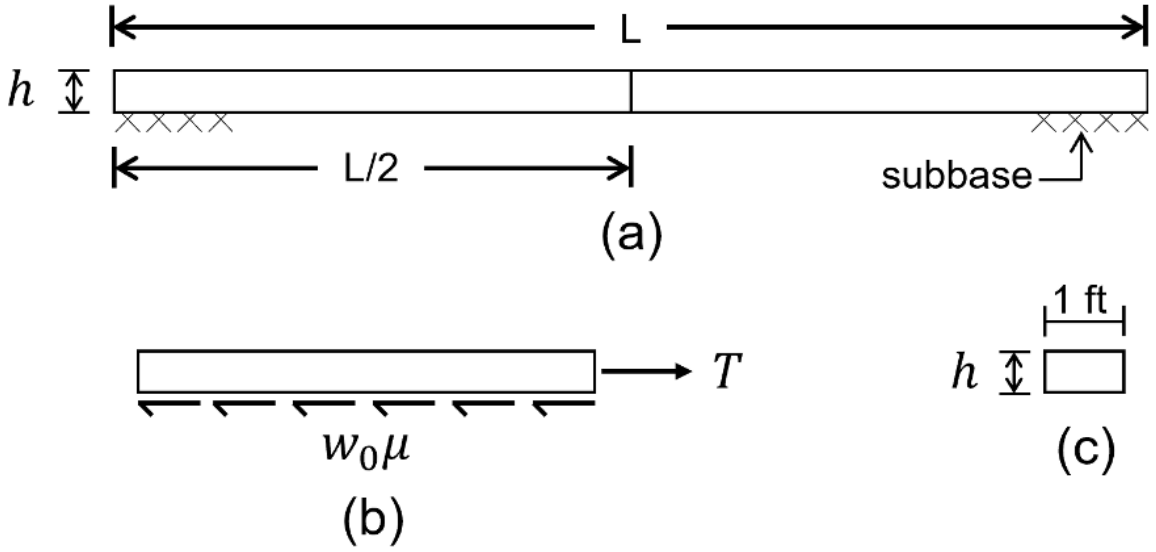

Fig. 2 Subbase drag effect: (a) Slab segment between joints;
(b) Equilibrium of horizontal forces; and (c) Cross-section view

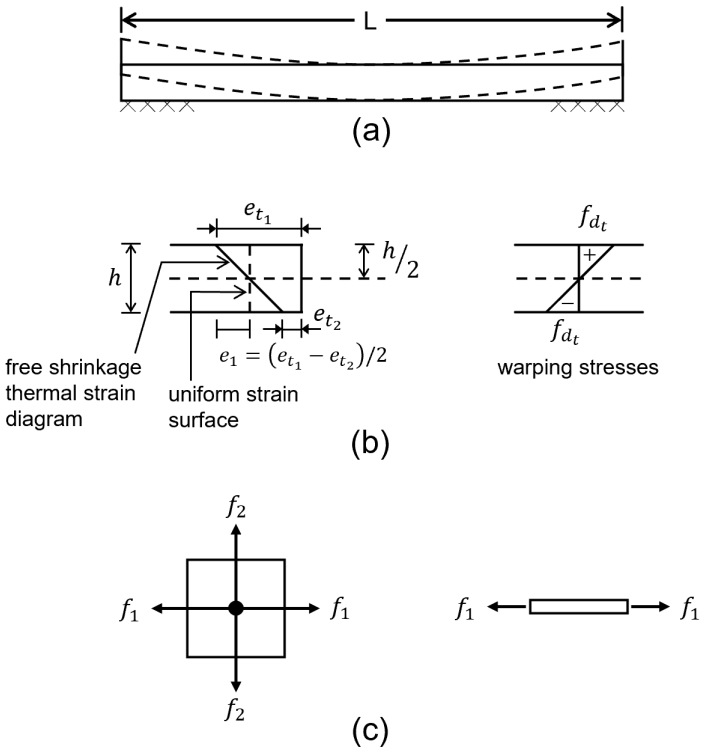

Fig. 3 Effect of differential temperature or shrinkage: (a) Warping of slab; (b) Strains and warping stresses; (c) Biaxially stressed element at the top surface of the slab

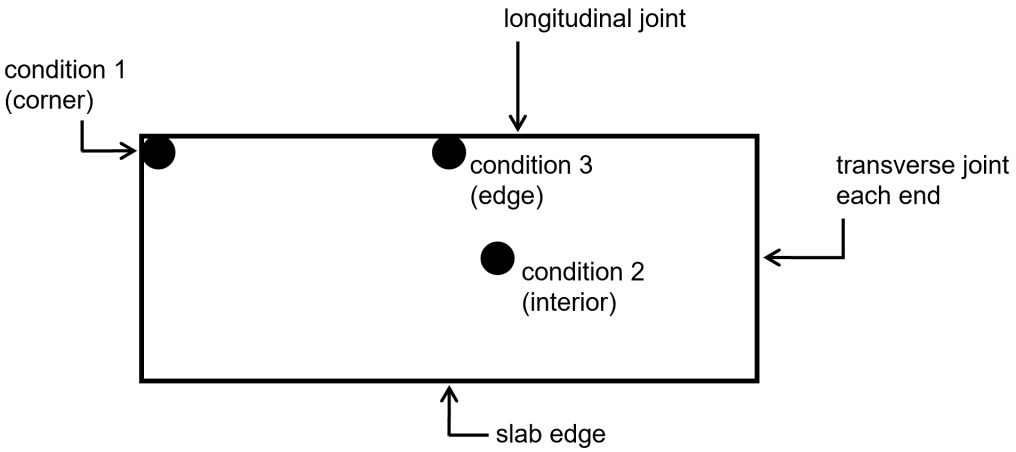

Fig. 4 Concentrated load conditions to be considered

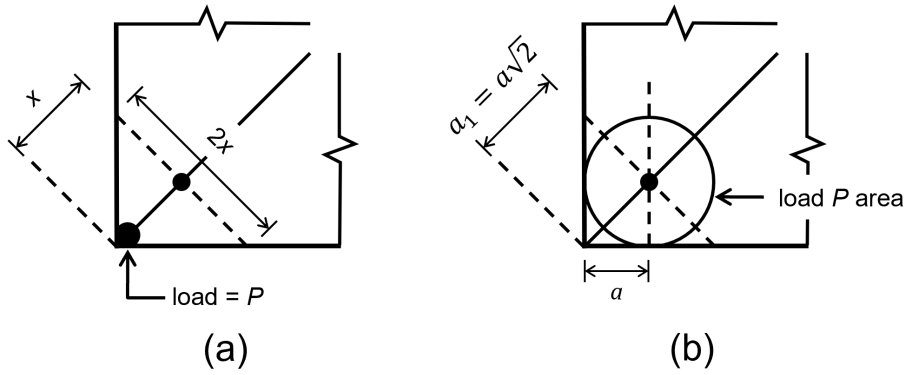

Fig. 5 Corner load in ground supported slab (a) considering that the area of load application is a point; and (b) considering a contact area of load application of radius *a*

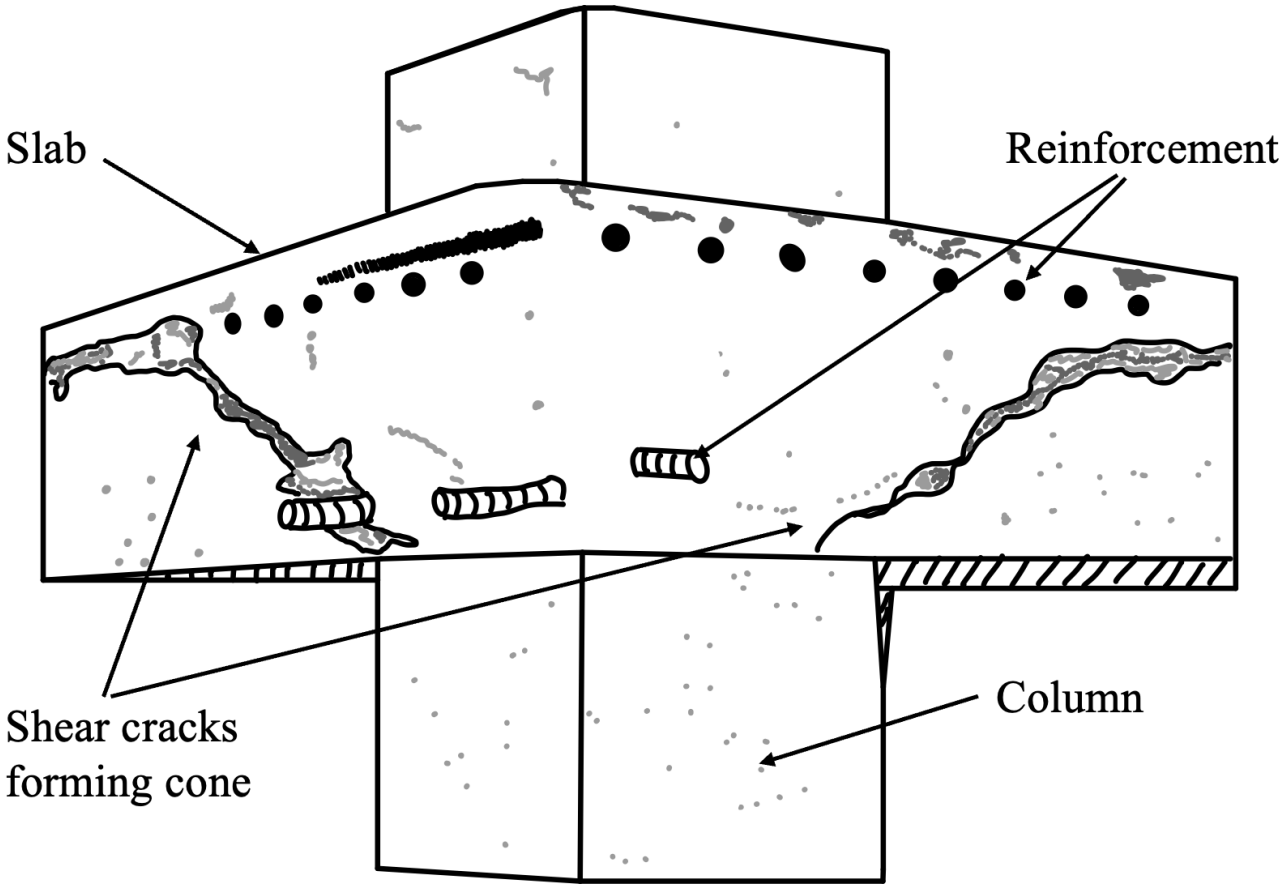

Fig. 6 Inclined cracks in a slab after a shear failure (image inspired by [40])

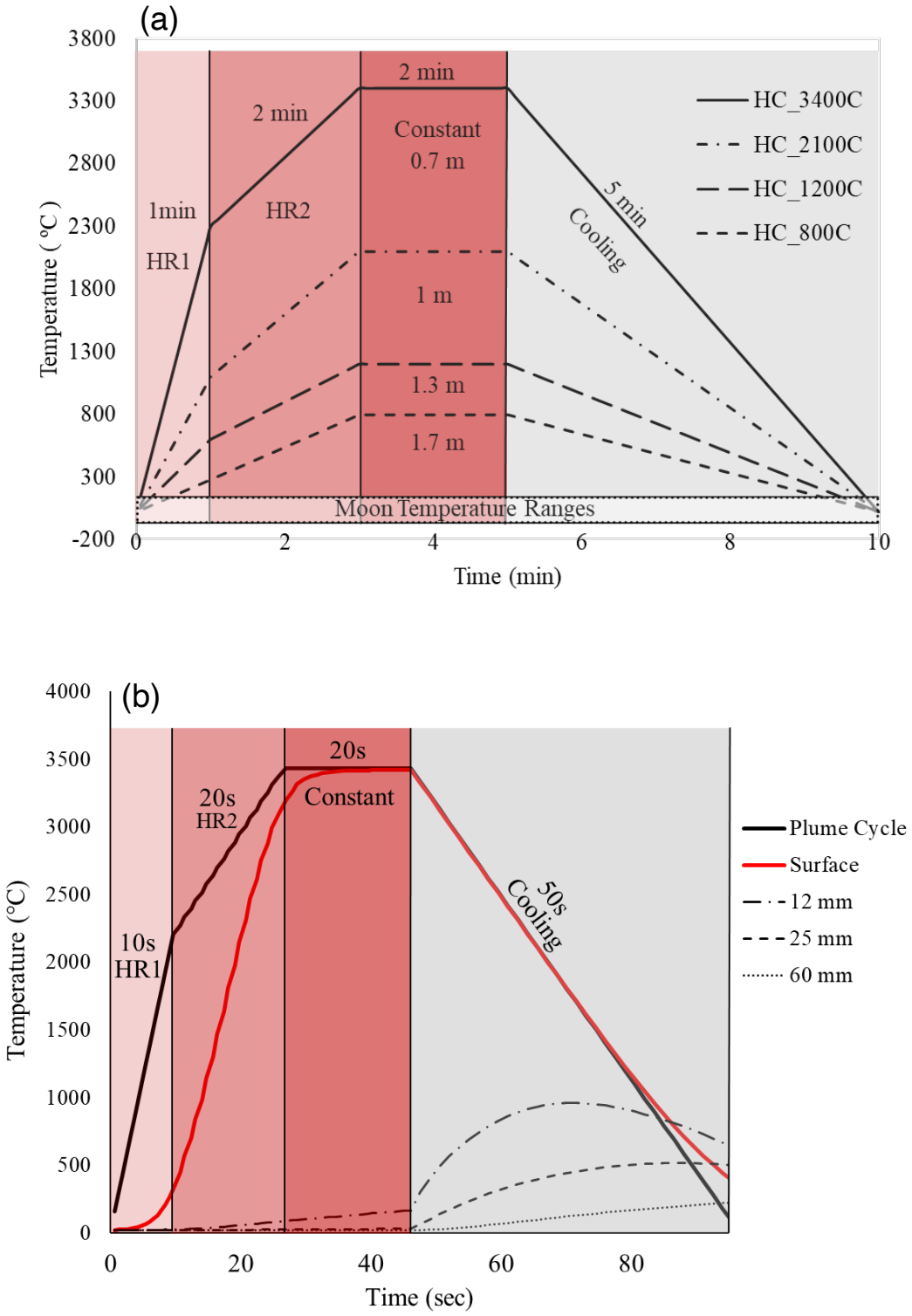

Fig. 7 Surface temperature boundary conditions implemented over time for launch condition (a) worst case, (b) more typical

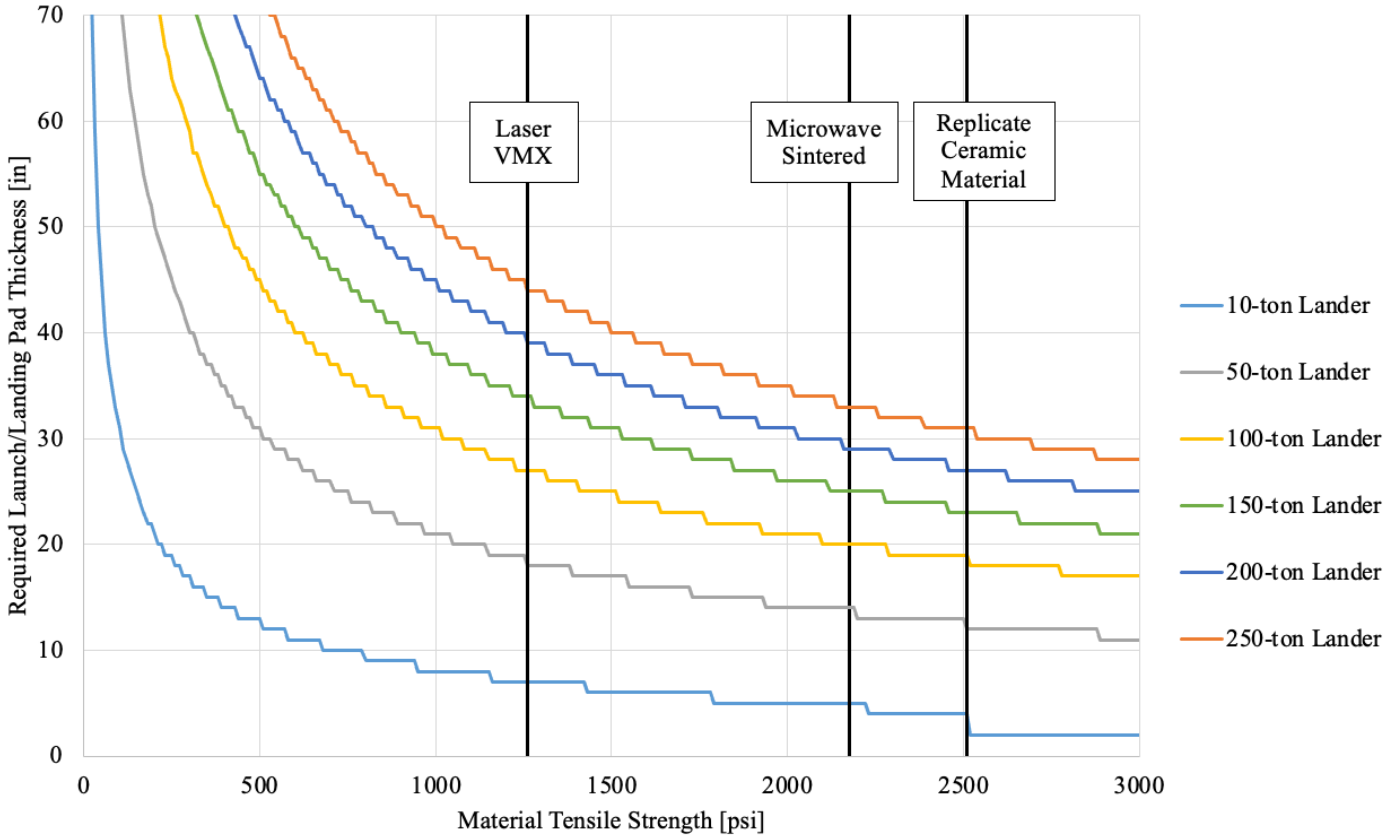

Fig. 8 Thickness required to prevent flexural cracking as a function of the tensile strength using an allowable stress of 2/3 the tensile strength (rounded up to nearest inch)

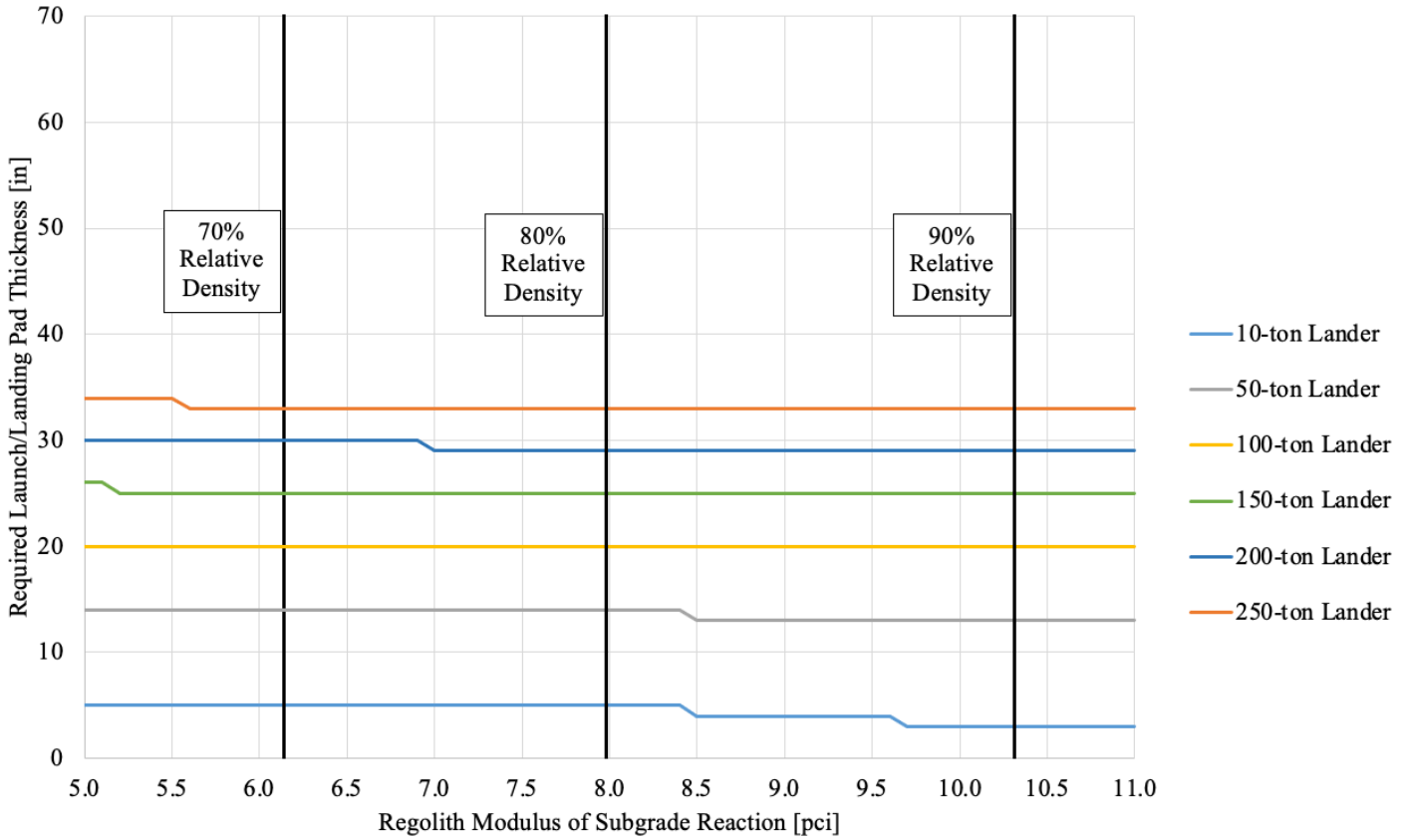

Fig. 9 Thickness required for various values of *k* with microwave sintered material

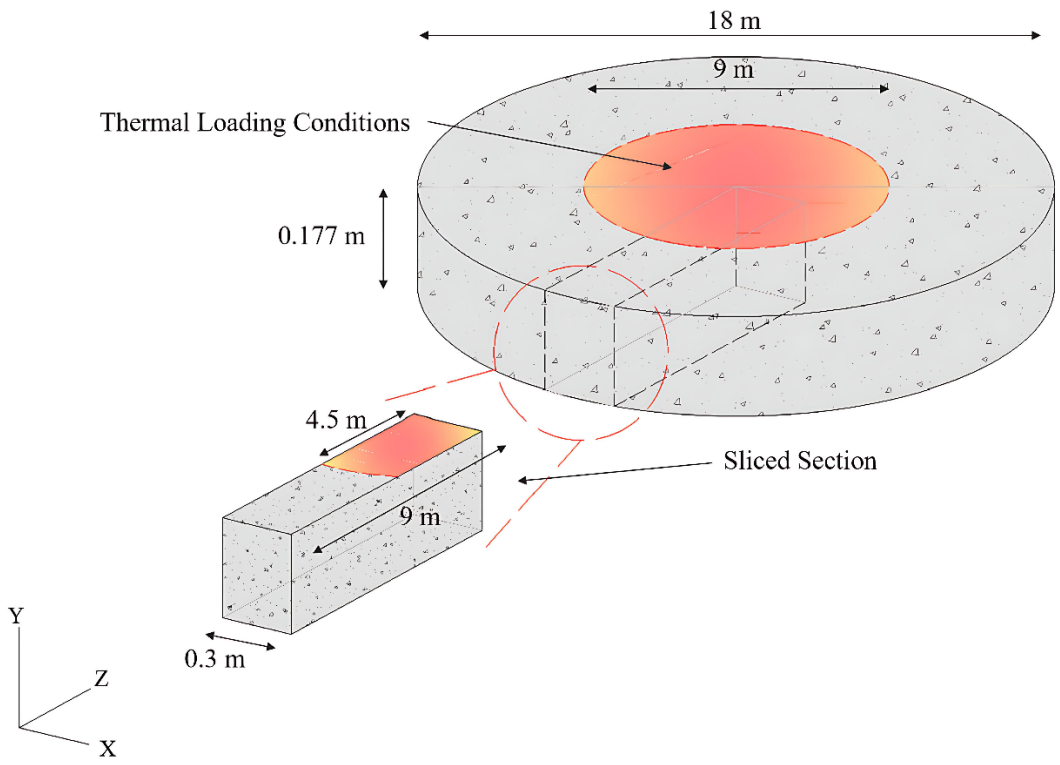

Fig. 10 Illustration showing a slice of the LLP model developed in MASA (not-to-scale)

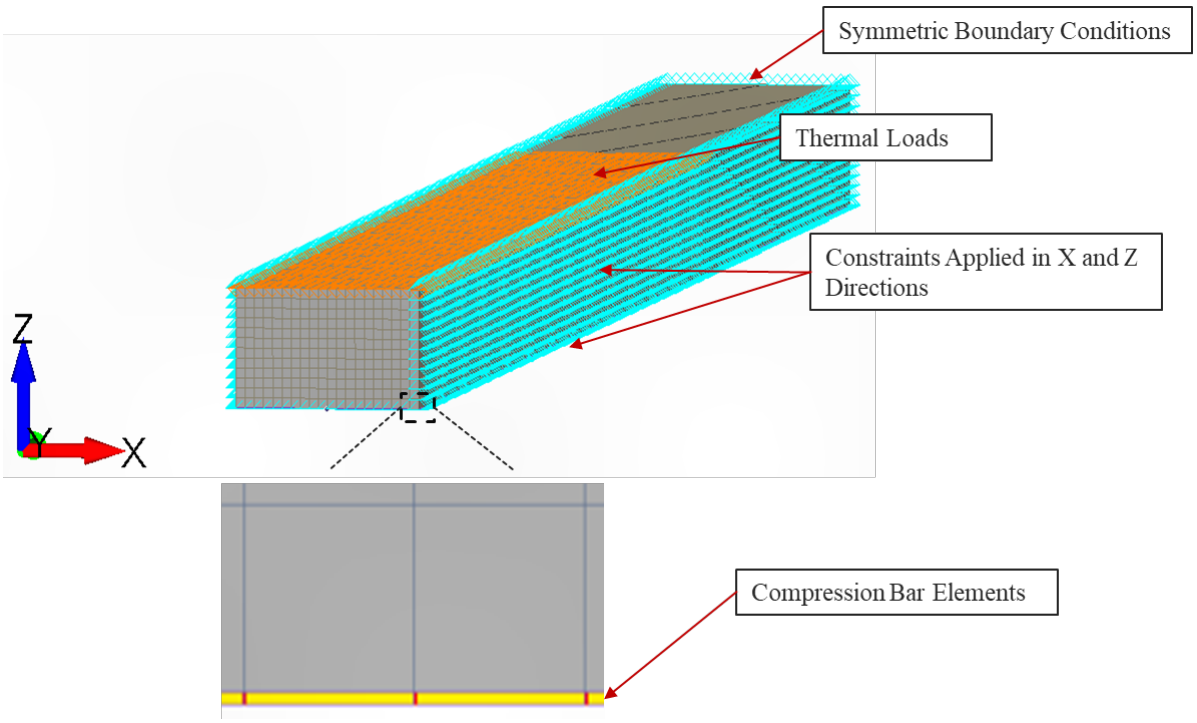

Fig. 11 Model of the sliced LLP showing the boundary conditions and thermal load conditions, as well as compression bar elements shown near the bottom surface of the pad

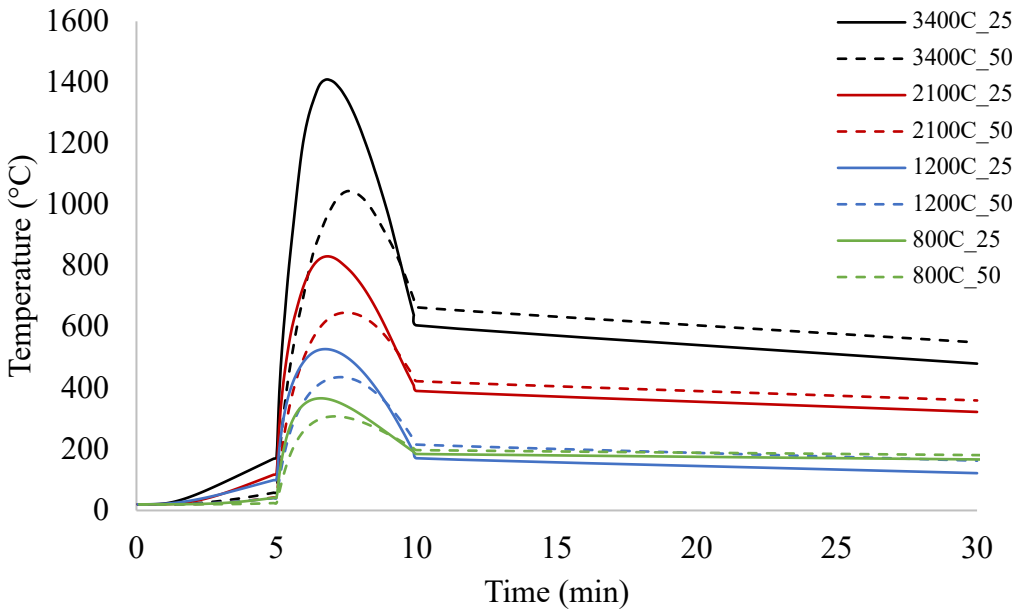

Fig. 12 Temperature inside the LLP at a depth of 25 mm (solid) and 50 mm (dashed) for various load cases

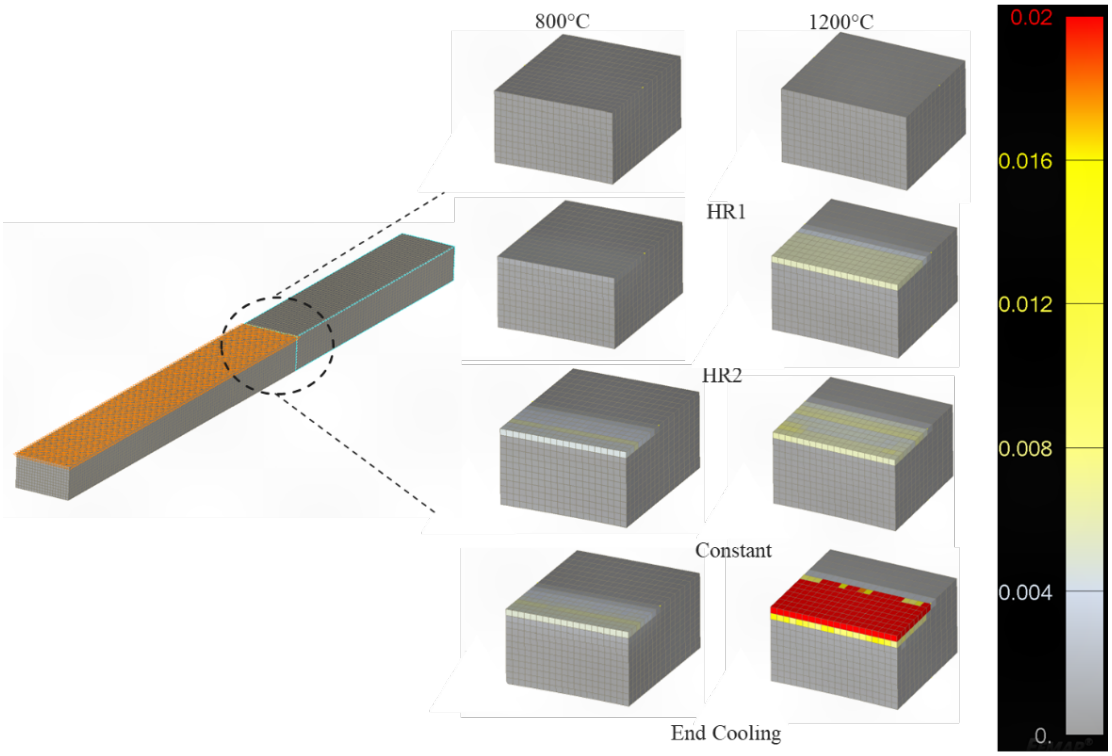

Fig. 13 Mechanical strains for 800°C and 1200°C load cases with a 0.02 maximum strain

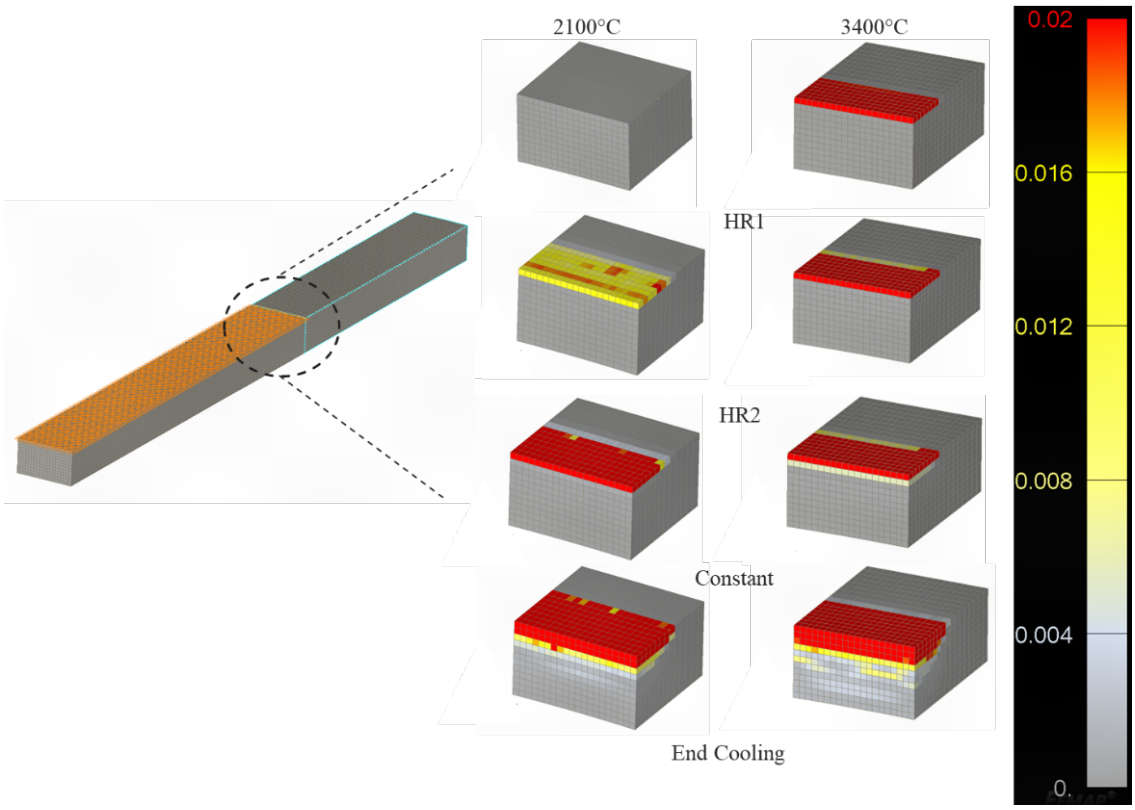

Fig. 14 Strains corresponding to a 0.3 mm crack width for a 15 mm element size for thermal load cases, 2100°C and 3400°C, respectively

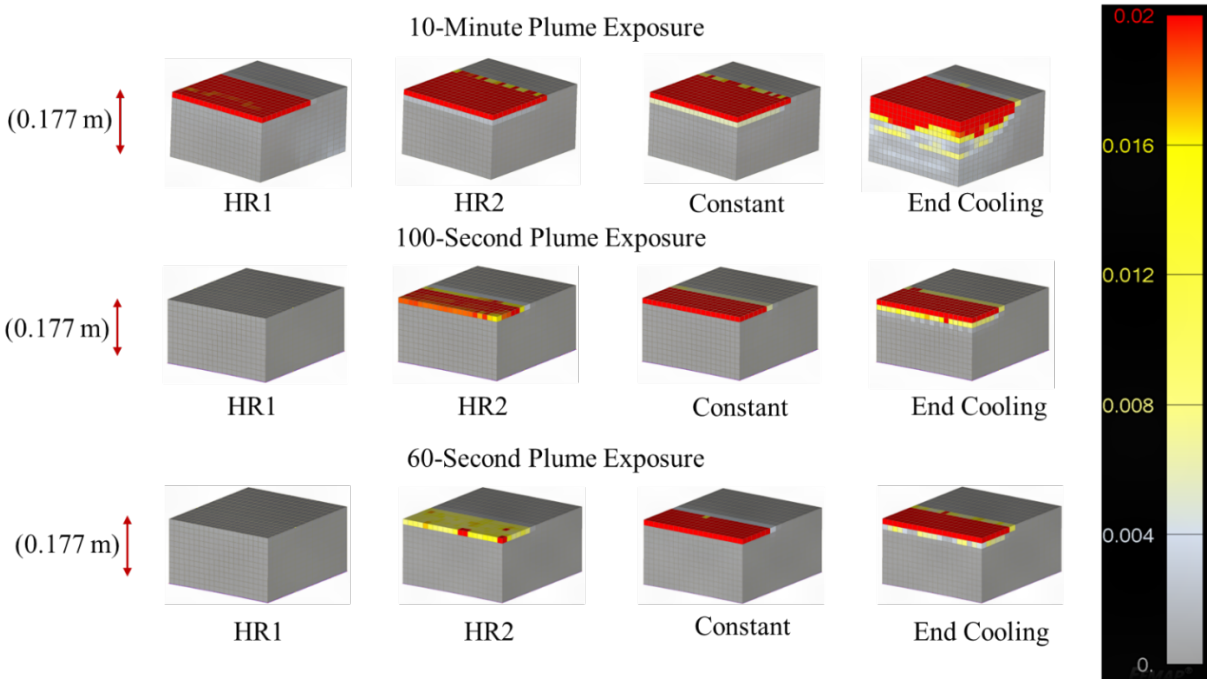

Fig. 15 Mechanical strains for 10 min, 100 sec and 60 sec plume exposure with a 0.02 maximum strain